Renewable and Sustainable Energy Reviews 41 (2015) 454–472

Contents lists available at ScienceDirect

Renewable and Sustainable Energy Reviews

journal homepage: www.elsevier.com/locate/rser

Designing large arrays of tidal turbines: A synthesis and review

Ross Vennell [a,*], Simon W. Funke [b,c], Scott Draper [d], Craig Stevens [e], Tim Divett [a,e]

[a] Ocean Physics Group, Department of Marine Science, University of Otago, Dunedin, New Zealand
[b] Department of Earth Science and Engineering, Imperial College London, UK
[c] Center of Biomedical Computing, Simula Research Laboratory, Norway
[d] Centre for Offshore Foundation Systems, University of Western Australia, Australia
[e] NIWA, Wellington, New Zealand

ARTICLE INFO

Article history:
Received 14 April 2014
Received in revised form
30 July 2014
Accepted 6 August 2014

Keywords:
Tidal stream energy
Resource assessment
Farm design

ABSTRACT

Much of the global tidal current energy resource lies in the accelerated flows along narrow channels. These channels have the potential to produce 10–1000 s of MW of electricity. However, realizing 100 MW of a channel's potential is much more complex than installing 100 1-MW turbines because large scale power extraction reduces tidal currents throughout the channel, changing the resource. This synthesis and review gives an overview of the issues and compromises in designing the layout of the large tidal turbine arrays required to realize this potential. The paper focuses on macro- and micro-design of arrays. Macro-design relates to the total number of turbines and their gross arrangement into rows, while micro-design adjusts the relative positions of the turbines within a grid and the spacing between rows. Interdependent macro-design compromises balance the total number of turbines, array power output, the power output of each turbine, the loads the turbines experience, turbine construction costs, maintaining navigability along the channel and any environmental impacts due to flow reduction. A strong emphasis is placed on providing physical insights about how "channel-scale dynamics" and the "duct-effect" impact on the compromises in array design. This work is relevant to the design of any "large" array which blocks more than 2–5% of a channel's cross-section, be it 2 turbines in a small channel or 100 turbines in a large channel.

Contents

⁎ Corresponding author. Tel.: +64 3 479 8307.
E-mail address: ross.vennell@otago.ac.nz (R. Vennell).

http://dx.doi.org/10.1016/j.rser.2014.08.022
1364-0321/

1. Introduction

Power generated from tidal currents could make a significant contribution to the global demand for renewable energy. Most of this resource lies in the concentrated energy of flows along narrow tidal channels [1–6]. The power which can be extracted from a channel is limited by tidal dynamics [7, hereafter GC05]. This limit, or "potential", ranges from Mega Watts for small channels, to Giga Watts for large channels. To realize this potential large arrays of tidal turbines must be installed within many channels, so as to cumulatively make a significant contribution to global demand. However, turbines within large arrays perform very differently to isolated turbines [8]. Together the works [9, hereafter V10, 10,11,8] demonstrate that, for large arrays there is no simple relationship between the total installed capacity of the turbines in the array and the array's total output, because the output of an individual turbine depends on the size of the array, how the turbines are arranged and the channel they are installed in. Importantly, the output of each turbine determines how many turbines are required to produce a given total array output, which strongly affects the cost of building an array [8].

This paper gives an overview of some of the issues and compromises involved in designing the arrangement of tidal turbines within large arrays. These complex issues extend to the gross design specifications for loads on the turbines and their output, which change as an array grows [11]. A clear understanding of these large array issues is critical at a time when tidal current power is about to move beyond the deployment of single turbines to deploying arrays of turbines. This understanding is also critical to those assessing the tidal stream resource available at numerous proposed array sites in order to determine how much power can realistically be produced from a site.

The large tidal turbine arrays required to realize a significant fraction of a channel's potential are very different to similarly sized wind turbine farms. While wind farms are too small to affect the weather systems which drive air past their blades, tidal turbine arrays must reduce tidal flows throughout the channel in order to realize a significant fraction of its potential, see Section 2.2. These large arrays are ones which can affect "channel-scale dynamics" or have the power coefficients of their turbines enhanced by the "duct-effect" [8]. The interaction of channel-scale dynamics and the duct-effect leads to key "array-effects" which are relevant to array and turbine design, see Section 2.1. A large array does not necessarily have a large number of turbines, see Section 2.6. Two turbines in a small channel are a "large" array, if they extract a significant fraction of its potential. Conversely, 100 1-MW turbines in the 100 km long Cook Strait NZ would be a "small" array because the Strait's potential is huge, 14 GW [5].

Threads within this synthesis and review address four questions (1) how do we arrange and tune turbines within large arrays to maximize array output? (2) how does the array layout affect the output per turbine, structural loads and construction costs? (3) how do we model and tune large arrays? and (4) what physical insights are relevant to developing a language which can be used to discuss large arrays? These threads are intertwined, e.g. our ability to investigate beneficial turbine arrangements is limited by the computational effort required to model and optimize large arrays. This computational effort is significantly increased because turbines must be "tuned" for a particular channel and array layout, in order to maximize array output [11].

The design of an array's layout has profound impacts on the number of turbines required to realize a given power output, the turbine designs required to withstand loads and their construction costs [11,8]. The array layout may also be constrained by water depth or local bathymetry. It is also likely constrained by the need to maintain navigation along the channel for vessels and marine life, and by the need to keep the flow reduction due to power extraction small enough to minimize environmental impacts, such as changes in sediment transport [12,13]. All of these aspects impact on array and turbine design, resulting in many compromises. Designing large arrays in channels is complex and warrants a review of the interplay between the array power output, turbine output, navigability and flow reduction, with the number of turbines in the array and their arrangement, loads and design specifications.

This review does not extend to the detailed design of turbines, e.g. blade design and tip speed ratios, but provides gross specifications for the output and loads that a turbine must meet to realize the estimated power production, along with some of the issues and compromises in designing the layout of turbines within large arrays. This work deliberately focuses on sites within tidal channels, as these hold much of the global potential. Other types of sites, such as headlands on open coastlines [14], arrays far from any coastline [15] or arrays near the shoreline [16] require further work.

For grid arrays of turbines the first major decision is the gross or "macro" array design. Macro-design decisions relate to the total number of turbines in the array, how many are placed in each row across the channel and how many rows to install, see Section 4. In contrast, "micro" array design exploits adjustments of the relative positions of the turbines within the grid to boost array output, see Section 5. Macro-design is about the total number of turbines required to produce a given power output, thus has a much larger impact on array and turbine output than micro-design. Consequently, macro-design will be addressed first with a synthesis of some of the compromises in arranging turbines within tidal turbine arrays (Section 2).

Designing both macro- and micro-arrangements of turbines within arrays requires hydrodynamical models, which require additional compromises in order to make them computationally feasible. Thus, this paper requires 3 interrelated mini-reviews (i) approaches to modeling arrays and optimizing the turbines within them (Section 3), (ii) macro-design of arrays (Section 4), and (iii) micro-design of arrays (Section 5). The synthesis and

review structure is used to allow the non-specialist to gain the important ideas from the synthesis, which is given first. Whereas the specialist can delve further to the three subsequent review sections to better understand the works which underpin the synthesis. Some sections of this paper are new work and are marked with an "⁎". This new work develops some of the language to discuss large arrays (Section 2.2), gives a schematic for macro-design compromises (Section 2.5), quantifies when an array is large (Section 2.6) and presents a basic metric for assessing the relative economic performance of turbines in arrays (Section 6.2).

The distinction between the macro- and micro-arrangement of grids of turbines, between large and small arrays, as well as the distinction between channel and non-channel sites, is artificial and partly driven by computational limits on modeling arrays of turbines, see Section 3. These limits have restricted array design to regular grids of turbines. However, real sites in channels or near headlands have complex tidal flow patterns, thus the optimal design is unlikely to be a regular grid. Thus new approaches to optimizing array designs are needed which integrate macro- and micro-design, see Section 6.1.

2. Compromises in macro-design of large arrays: *synthesis*

It is important to be clear that there are two aspects of power production which have a bearing on the economics of developing an array within a channel (1) the array's total output and (2) the output from each turbine. The total power output determines the income from the array. The power output by each turbine determines the number of turbines required to achieve a given array output and the structural loads they experience, thus affects both array and turbine construction costs. For large arrays there is no simple relationship between how much the array's power output increases and how much the individual turbine's output increases, as new turbines are added to a farm [11]. Large arrays are ones where the area swept by the turbines occupies more than 2–5% of a channel's cross-sectional area, see Section 2.6

2.1. Key "array-effects"

There are a few key results about the dynamics of turbines within large arrays which are critical to understand power production. They are also needed to understand why there are compromises in designing array layout (Section 2.5) and in making the modeling of tidal turbine arrays computationally feasible (Section 3). These key dynamical array-effects are given below, while their consequences are discussed in Sections 2.2–2.6 and Sections 3–5.

1. *Power extraction by a large array reduces the free-stream flow throughout a channel*: This interaction between the power extraction and the tidal current resource makes estimating the resource in the numerous narrow tidal channels which hold much of the global potential complex [GC05, V10].
2. *There is a maximum power which can be extracted from a channel, its "potential"*: This maximum results from a balance between increasing a farm's gross drag coefficient in an attempt to increase power production and the associated reduction in the free-stream velocity which reduces power production. To realize most of a channel's potential requires most of the cross-section of the channel to be filled with turbines [GC05, 11].
3. *Turbines within arrays require an individualized tuning which is specific to the channel, the array size and the turbine arrangement*: Tuning comes at a high computational cost. The need for individualized tuning arises because turbines in channels interact with each other, even if they are so far apart that their wakes do not impinge on each other. This interaction results from the enhanced drag due to power extraction by a turbine, reducing the free-stream flow for every turbine in a channel [V10, 10,11], Section 3.2, Fig. 5.
4. *Optimally tuned turbines in large arrays perform very differently to tuned isolated turbines*: For example, they may have optimal power and thrust coefficients much higher, or lower, than at the Betz limit. Individual turbine performance depends on the number of turbines, how they are arranged into rows and the size and dynamical balance of the channel [10,8,16,17], Section 4.1, Fig. 5.
5. *The power return on adding turbines to a row within a large array may increase or decrease, depending on the characteristics of the tidal channel*: There is an increasing power return on turbines added to rows in moderately-large arrays in large channels. i.e. an increased output for each individual turbine. In contrast, individual turbine output falls when turbines are added to rows of arrays in small channels, i.e. a diminishing return on additional turbines. Large channels are deeper ones where the flow's inertia is significant in the undisturbed channel. Small channels are shallower ones where natural bottom friction dominates the dynamics of the undisturbed channel [GC05, V10, 11], Section 4.2, Fig. 6.
6. *There is a diminishing power return on rows of turbines added to an array*: Adding rows of turbines to arrays in both large and small channels decreases the individual output of all turbines within the array, even though it may increase total array output. This diminishing return means that more turbines are required to realize a given array output [18], Section 4.3, Fig. 7.
7. *Loads on the turbines and construction costs are related to the power output of each individual turbine*: An increasing power return on additional turbines means a higher individual turbine output, which also results in higher structural loads. Thus turbines must be more robust, increasing the construction costs of each turbine. Conversely, a diminishing power return on additional turbines is partially offset by allowing all turbines to be more lightly built, reducing turbine construction costs. [8]
8. *It is possible to boost turbine output by adjusting their relative positions within a grid array*: These micro-design options for regular grids of turbines include "packing" turbines together in the cross-stream direction or "staggering" turbines in one row relative to those in an upstream row [19–21,17], Section 5. These benefits exploit the interaction of turbine wakes.

Array effects #1–#7 apply to large arrays within channels. Array effect #8 applies to both large and small arrays, in channel and non-channel sites, e.g. [14].

There is another recently demonstrated array-effect not discussed here. Most research to date has optimized a farm drag coefficient which is constant in time. However, optimizing how the farm drag coefficient varies during a tidal cycle allows an array to temporarily store energy. In large channels this "inertial-storage" array-effect enables arrays that are large enough to reduce the free-stream flow to benefit from manipulating the phase of that flow. Inertial-storage can also be used to exceed GC05's upper limit, array-effect #2, while maintaining stronger flows within the channel, or to better meet predicable peaks in power demand [22].

2.2. ⁎ "Channel-scale dynamics" and the "Duct-effect"

Array-effects #1–#7 are the result of two competing effects. The first is the effect that the array has on "channel-scale dynamics". When an array becomes large enough to influence channel-scale dynamics power extraction that reduces the free-stream flows

experienced by all turbines. Despite turbines superficially extracting energy from tidal currents along the channel, the array's energy source is actually the finite head loss between the ends of the channel which drives these tidal currents, Fig. 1b. This head loss is a result of larger scale tidal patterns in the water bodies connected by the channel. The finite head loss is the reason that the additional drag due to power extraction reduces free-stream flows throughout the channel and also limits array output, array-effect #1 and #2.

The second competing effect is due to the channel forming a partial duct around the turbines. This “duct-effect” enhances turbine thrust and power coefficients, changing the performance of turbines within the array [23,8]. Array-effects #3–#7 are the result of the interaction of these two competing effects. This interaction produces different array-effects depending on the size of the array and the size of the channel because the effect of the array on channel-scale dynamics differs for large and small channels due to the differing importance of background bottom friction in their dynamical balances [18].

2.3. Macro-design of arrays

The macro-design, i.e. the total number of turbines and their gross arrangement into rows, Fig. 1, has a much larger impact on the array and individual turbine outputs than micro-design which is reviewed in Section 5. Thus, macro-design largely determines the power output of the array and of individual turbines, and can be used to give gross estimates of the array's total power output and the structural loads on the turbines.

To discuss macro-array design this paper uses two examples to illustrate macro-design considerations in two very different tidal

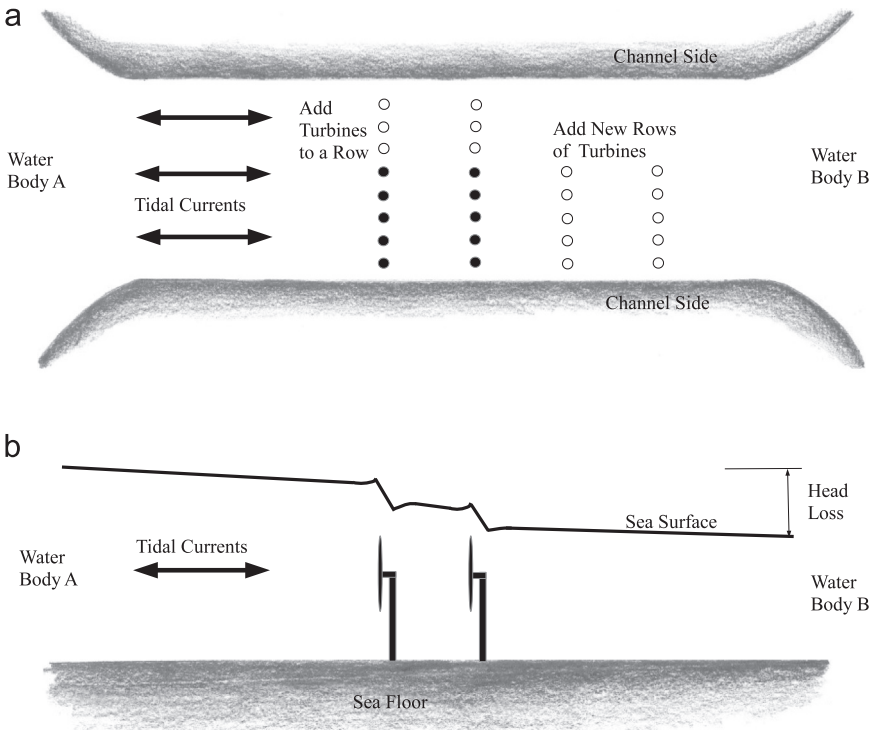

Fig. 1. Schematic diagram of tidal turbine array in a channel connecting two large water bodies. (a) Two ways of expanding an array, adding turbines to the rows or adding new rows of turbines. (b) Vertical slice through array showing exaggerated changes in sea level, see [17].

Table 1
Example channel loosely based on the Pentland Firth and a hypothetical small channel. λ_0 is a non-dimensional measure of the importance of background bottom friction and α is a non-dimensional measure of the distance traveled by a water parcel in half a tidal cycle [18].

	Pentland firth UK	High flow small channel
Length, L	20 km	2 km
Width, W	9 km	0.5 km
Depth, h	50 m	20 m
Bottom drag coefficient C_D	0.025	0.0025
Undisturbed free-stream velocity, u_{UD}	2.7 m/s	2.7 m/s
Peak turbine output in undisturbed velocity, or first turbine	2.1 MW	2.1 MW
Head loss amplitude, Δ	0.9 m	0.17 m
$\alpha = 8\, g\Delta/3\pi\omega^2 L^2$	1.0	18
$\lambda_0 = \alpha C_D L/h$	1.0	4.6
Average potential	2.3 GW	9 MW
Peak flow potential	5.5 MW	21 MW
Reduced free-stream velocity at potential	1.5 m/s	1.4 m/s
400 m^2 turbines required to fill cross-section	1100	21

channels, see Table 1. A channel loosely based on the Pentland Firth is used as an example of a large channel where the flow's inertia is important within its dynamical balance. Strong tidal currents flow through the Firth, which lies to the south of the Orkney Islands. These currents have a potential for up to 4 GW of tidal current power generation [24,6,25]. The Firth has several islands and connected channels, is around 23 km long and around 70 m deep and maximum flows can exceed 4.5 ms^{-1} in some locations at spring tides. Tables giving more details about the Firth and its generation potential are given in [6,25,8,22].

A second hypothetical example in used to illustrate array design in small shallow channels where background bottom friction dominates dynamics. This small channel is 2 km long, 500 m wide and 20 m deep, with maximum tidal flows of 2.7 ms^{-1} and a potential to produce up to 9 MW of electricity. More details of this small channel and its power generation capacity are given in [10,11].

To estimate the number of turbines required to produce a given array output, a turbine with the same 400 m^2 swept area as the Seagen is used [26]. Unlike the Seagen, the turbines used here have no limits placed on their output. Thus the given number of turbines should be viewed as the minimum number required to produce a given array output. The simple 1D model for a short narrow channel connecting two large water bodies [27,18] is used to make it computationally tractable to explore the 1000 s of arrays required to give an overview of the macro-design of large arrays. While the 1D model can be used to scope the size and arrangement of large arrays, it requires more work to address its limitations, see Section 7. More details about the example channels, example turbines and 1D model can be found in [5,10,18,11,8].

2.4. Array and turbine power output contours

The necessarily complex Fig. 2 shows the two aspects of array power output relevant to the economics of large arrays, the array's total power output and the average power output per turbine, along with contours of the number of turbines in simple grid arrays. The figure demonstrates two ways to expand an array, adding turbines to existing rows or adding new rows of turbines. These expansions correspond to moving up and right respectively within the contour plots. The most important aspect of the figure is that the 3 sets of contours have different patterns, due to the differing degrees to which adding turbines to a row and adding rows of turbines affect array and turbine outputs. The differences in contour patterns necessitate macro-design compromises which trade off array output and individual turbine output.

The diminishing return on additional rows, array-effect #6, is seen as a decline in the output per turbine when moving left to right within both examples in Fig. 2. An increasing return when adding turbines to the rows in large channels like the Pentland Firth is seen in the increasing output per turbine when moving upwards in Fig. 2a within the light blue region, array-effect #5. For the small channel there is a decreasing power per turbine. i.e. diminishing returns, when moving both upwards and to the right within Fig. 2b, array-effects #5 and 6.

The arrays in both examples are large in the sense that they play a significant role in channel-scale dynamics or their turbine performance is affected by the duct-effect, see Section 2.6. However "large" can be divided into three sub-categories based on turbine and array performance. For the Pentland Firth, moderately large-arrays within the blue area benefit from turbines producing more power than an isolated turbine in the undisturbed free-stream flow, array-effect #4. This is possible because in larger channels with "moderately-large" arrays, the beneficial duct-effect

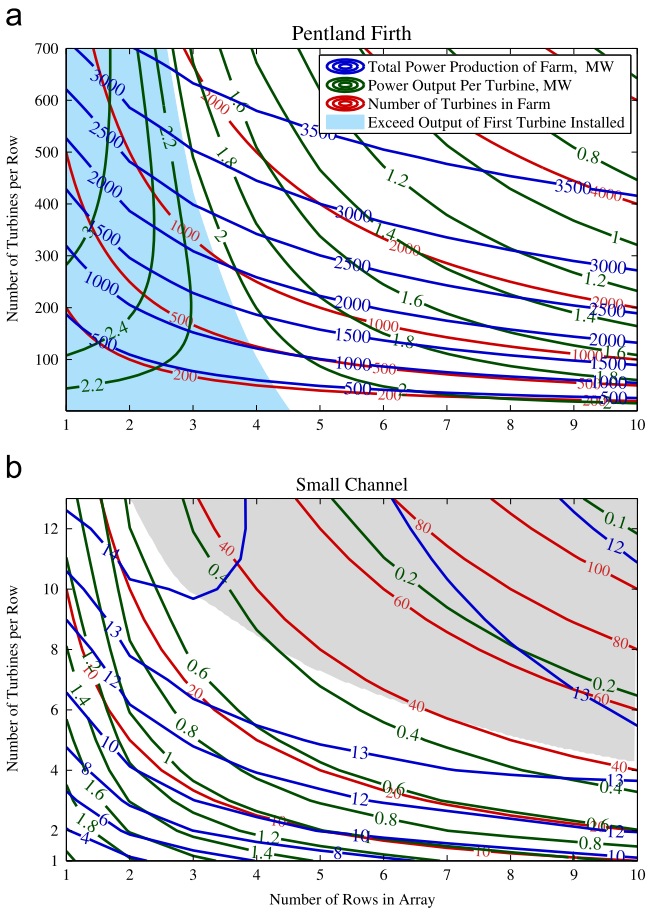

Fig. 2. Complex contour plots illustrating some of the compromises required in designing large arrays of tidal turbines in the two example channels. Blue contours give total power production by the array at peak flow, green contours the power output per turbine at peak flow and red contours indicate the minimum number of optimally tuned 400 m^2 turbines in the array. Arrays in the light blue region have turbines which each produce more power than a single isolated turbine. The gray area in the upper right of the small channel example is extremely-large arrays, where adding turbines reduces array output. (For interpretation of the references to color in this figure caption, the reader is referred to the web version of this paper.)

outweighs flow reduction due to channel-scale dynamics, array-effect #5. The second category is "very-large" arrays, representing arrays outside the blue area in the Firth and arrays in the lower left of the small channel's contour plot. These arrays have a diminishing return on both turbines added to a row and on additional rows, array-effects #5 and 6. For "very-large" arrays in small channels background bottom friction already extracts a large fraction of the flow's energy before any turbines are installed [18]. Consequently, flow reduction due to channel-scale dynamics dominates the duct-effect. The third category is "extremely-large" arrays, representing arrays within the gray area in the upper right of the small channel example. These arrays are so large that array output falls as turbines are added, thus they are outside the useful design space!

2.5. ⁎ A schematic of macro-design compromises

Fig. 3 gives a schematic representation of some of the compromises in the macro-design of large arrays which are inherent in the 3 sets of contours in Fig. 2. The first compromise is between total power production and the effects of a reduction in free stream flow due to power extraction. This 1 ↔ 2 compromise is not orientated at right angles to contours of the number of turbines in Fig. 2. This is because adding turbines to a row increases the power

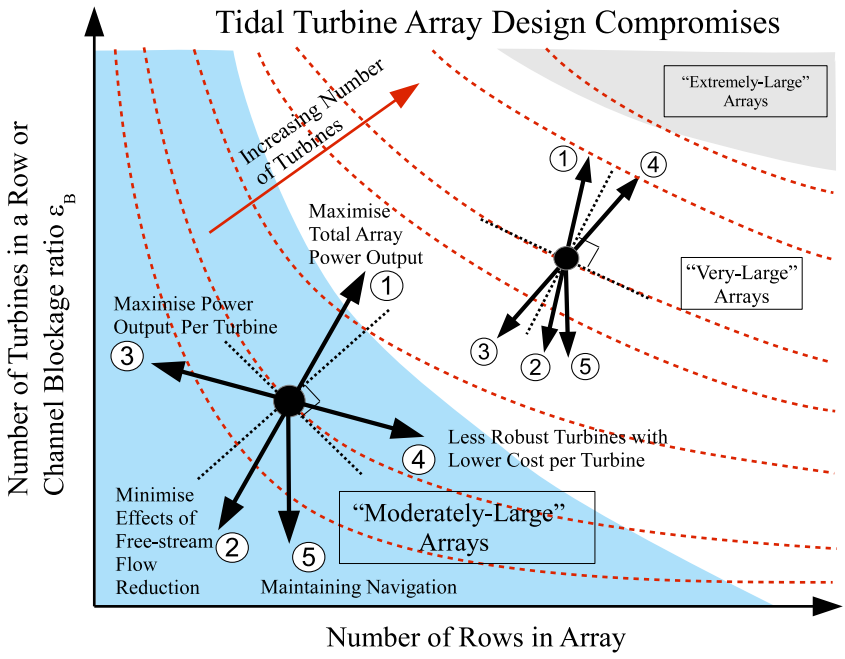

Fig. 3. A schematic diagram of the tidal turbine array macro-design compromises inherent in Figs. 2 and 8 for growing a farm within a channel by adding rows or by adding turbines to the rows, see Section 2.5. Arrays joined by a dashed red curve have the same total number of turbines. The two black dots are particular arrays with a given number of rows and turbines in each row. The black dashed lines are tangent and normal to the turbine number contour through the black dots. The black arrows represent effects which would pull the farm layout in that direction relative to the turbine numbers contours. In the blue region are "moderately-large" arrays where the power output per turbine exceeds that of the first turbine installed in the channel. For these arrays the duct-effect outweighs channel-scale dynamics. For arrays outside this area channel-scale dynamics outweighs the duct-effect. In the upper right are "extremely-large" arrays, for which adding turbines reduces array output. (For interpretation of the references to color in this figure caption, the reader is referred to the web version of this paper.)

produced by the array more quickly than adding additional rows. A second compromise is between the power produced by each turbine and the cost of building the turbines. This 3↔4 compromise in Fig. 3 is between having fewer highly productive, more robust, costly turbines and more less productive, more lightly built, cheaper turbines.

Another compromise is between maintaining navigation along the channel, direction 5, and the combination of power production per turbine and total power production. Maintaining navigation requires a smaller channel blockage ratio, whereas power production may have better economics at higher blockage ratios. The maximum blockage ratio will be set by a particular site's bathymetry, vessel traffic, and environmental constraints.

For arrays within the light blue region of Fig. 2 the 3↔4 compromise is oriented roughly NW–SE, the exceptions are the arrays on the extreme right of the light blue area. Therefore, for these "moderately-large" arrays adding turbines to the rows increases both the total power production and the power output per turbine, array-effect #5, while also increasing the cost of building those turbines to withstand higher loads, array-effect #7. For "very-large" arrays, those outside the light blue area the 3↔4 compromise is roughly oriented SW–NE. Thus, both adding turbines to a row or adding rows in these very-large arrays reduces the power per turbine, while at the same time increasing the array output from a larger number of more lightly constructed and cheaper turbines. For "extremely-large" arrays in the upper right, adding turbines also reduces the array's total output, thus such arrays would not be built.

Except for a few particular array layouts, none of the compromise directions in Fig. 3 are at right angles to each other. Thus, it is generally not possible to change the layout of the array by moving along any of the five directions without affecting all of the other compromises. Thus the compromises are interdependent. To resolve these interdependent compromises requires more detailed economic information, such as the cost of producing turbines to withstand a range of loadings, the income from power production or estimates of the environmental costs in dollars associated with given flow reductions. While Section 6.2 suggests a turbine benefit-to-cost ratio which provides a mean to quantify the 3↔4 compromise, the costs required to quantify environmental and other compromises may not be readily available. Thus, the compromise diagram Fig. 3 is mainly conceptual, but does provide a useful framework for designing the layout of tidal turbine arrays.

2.6. ∗ When is an array large?

It is important to answer the technical question, when is an array large? This review takes a physical view of large arrays. A large array is one which is able to influence channel-scale dynamics or one where the channel alters turbine performance via the duct-effect. Conversely a "small" array is one too small to influence channel-scale dynamics and where the individual turbines each perform almost as though they are far from other turbines and the sides of the channel. Specifically here, a "large" array will be taken as one, where due to the duct-effect, the power output per turbine differs by more than 5% from that of an isolated turbine operating in the free-stream flow of the undisturbed channel. Or, one where the total force on the array, see Eq. (1) below, is more than 5% of the forcing due to the head loss between the ends of the channel, thus the array is influencing channel-scale dynamics. A 5% threshold was chosen because other significant improvements to array output due to packing or staggering are in the 5–20% range, Section 5.

Fig. 4a uses the 1D model to give the minimum channel blockage required for an array to meet one of the 5% thresholds. The channel blockage ratio ϵ_B is simply the fraction of the channel's cross-sectional area which is swept by the blades of the turbines in one row. This minimum ϵ_B depends on two non-dimensional numbers defined in Table 1. The first λ_0 gives the importance of background bottom friction within channel-scale dynamics. The second α can be

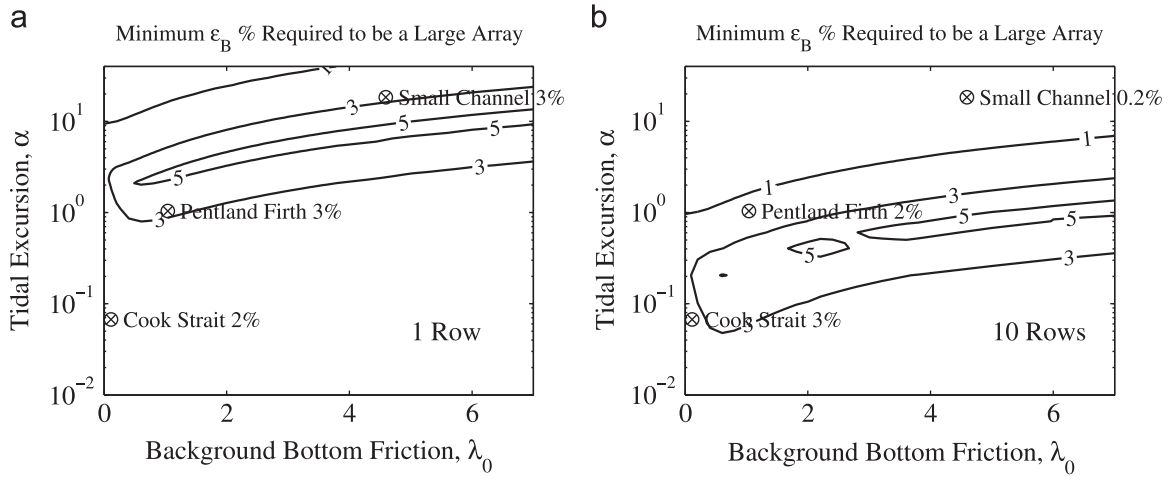

Fig. 4. Minimum channel blockage ratio required to be a large array from the 1D model. Contours give the ϵ_B required, as a percentage, to change the power output per turbine by 5% relative to the output of an isolated turbine operating in the undisturbed flow, or for the total force on the array to be 5% of the forcing due to the head loss between the ends of the channel. The array has (a) a single row or (b) 10 rows of optimally tuned turbines across the channel in a uniform grid. Horizontal axis is the relative importance of bottom friction in the channel-scale dynamics, λ_0. Vertical axis is the distance traveled by a water parcel in half a tidal cycle, the tidal excursion, relative to the length of the channel, α (see V10 and Table 1).

interpreted as how far a water parcel moves in half a tidal cycle relative to the length of the channel, V10. For the Pentland Firth a blockage ratio $\epsilon_B = 3\%$ is sufficient for an array to be large. In the much larger Cook Strait NZ, bottom friction is almost unimportant and $\epsilon_B \geq 2\%$ is required to be large. For the small channel, $\epsilon_B \geq 3\%$ is required. However, one 400 m^2 turbine has $\epsilon_B = 4\%$, thus all arrays in the small channel example are "large". The ridge in Fig. 4a corresponds to particular channels where the effects of the duct-effect and flow reduction due to channel-scale dynamics almost cancel each other, thus higher blockage ratios are required to exceed one of the 5% thresholds.

Fig. 4b gives the minimum ϵ_B to be a large array for arrays with 10 rows. This changes the contour positions when compared to those for a single row. However, the minimum ϵ_B is still typically in the range of 2–5% for most channels. Though the definition of a large array is technically complex, Fig. 4 demonstrates that a useful working definition is, "an array becomes large if the turbines block at least 2–5% of the channel's cross-section". The exact blockage depends on the size and dynamics of the channel and the number of rows in the array.

3. Modeling tidal turbine arrays: *review*

To both estimate the tidal energy resource available at a site and to design an array for that site it is essential to develop a hydrodynamical model. This section outlines the approaches to, and compromises in, modeling arrays of tidal turbines. The large arrays required to realize a significant fraction of a channel's potential will play a significant role within the model's dynamics. Thus firstly, the model must include turbines to account for the interaction between the power extraction and the strength of the tidal currents, array-effect #1. Secondly, the effects of the array extend well beyond its immediate vicinity, thus a large region around the array must also be modeled. It is not yet computationally feasible to construct a numerical model which is capable of both resolving the sub-turbine blade scale turbulence (≈ 0.01 m) which is generated as they turn, and span the 20–500 km of the coastal ocean around the site needed to model tidal patterns in the region. Thus the modeling of tidal turbines in arrays is separated into two distinct types (1) detailed 3D CFD models of a small number of turbines and (2) hydrodynamic models which incorporate large numbers of turbines using a coarse representation of the turbines. Both types of approach incur the additional computational cost of the many model runs required to tune their turbines to maximize output, array-effect #3.

3.1. CFD modeling of small arrays

At the small scale, detailed 3D CFD models can be used to predict hydrodynamic load distributions over individual turbine blades and the streamlines of the 3D rotating fluid within the turbine's wake, or flow separation around the turbine's blades [28,29]. A less detailed representation of a turbine, such as actuator lines or disks in a 3D CFD model [30,31] or using blade element theory [20,32], can model arrays with several turbines. However these detailed 3D CFD models require compromises to reduce the computational effort of modeling larger arrays of turbines, e.g. assuming the free-stream flow is fixed. They may also simulate a row of evenly spaced turbines by imposing periodic boundary conditions in the cross-flow direction, and simulate multiple rows of turbines by imposing periodic boundary conditions in the along stream direction [33–37]. Essentially these are using a 3D CFD model of one or more turbines within an elongated box to simulate part of a much larger array. Though the "multiple box" approach may simulate the "duct-effect", it is limited to modeling "small" arrays in straight channels unless it also models free-stream flow reduction, something not yet attempted with 3D CFD models. Detailed 3D CFD models with periodic boundary conditions of a small number of turbines can be used to understand the impact of one row on the next, which is useful in estimating minimum row spacing, and the advantages of other micro-arrangement strategies such as staggering rows, see Section 5. They are also useful in modeling the effects of turbine generated turbulence and wake recovery on down stream turbines, or the effects of acceleration of the free-stream flow due to free-surface effects [38,32]. However, the computational cost of detailed 3D CFD models of turbines precludes them being used to model large arrays in realistic coastal sites.

3.2. Modeling large arrays within a coastal tidal model

To model large arrays in coastal sites the model's domain must be sufficiently large that power extraction from the proposed site has a negligible effect on tidal currents at the model's boundaries and transients are able to escape through the boundaries [39–41]. The computational effort due to the disparity of scales between

the turbine and the size of the coastal model domain can be significantly reduced by using unstructured model grids and by using a depth averaged, or 2D, numerical model of the coastal region, rather than a 3D model. However, to be computationally tractable, models of large arrays within domains spanning 100 km or more of coastal ocean must use a simplified representation of the turbines. Simplification balances the computational effort off against the smallest scale of turbulence which is explicitly modeled. The smallest scale modeled is typically the sub-turbine scale turbulence ($\approx$1 m) for representations of individual turbines which are 10–20 m in size [42–44], or the sub-array scale turbulence (10–1000 m) for those modeling groups of turbines [45,46]. Models using simplified turbine representations still require some parametrization of turbulence on scales which are smaller than the smallest explicitly modeled scale.

A consequence of flow reduction due to power extraction is that model turbines need individualized tunings, which are specific to the channel and to the array design, in order to maximize the array's output, [10,11], array-effect #3. Thus the coastal models will need to be run many times in order to search for the optimal individualized tunings of the turbines for each array size and arrangement being investigated. The necessity for individualized tuning increases the computational effort to model large arrays by orders of magnitude [11]. Thus it is essential to make the representation of the turbines as simple as possible, while still modeling array scale effects.

How to incorporate simplified turbines into coastal models revolves around how the drag forces associated with power extraction are modeled. Essentially the aim is to "upscale" the effects of the detailed flow and turbulence around a simplified turbine to give a coarse representation of the hydrodynamic force on a turbine or a group of turbines. The force on the fluid due to power extraction by an array is typically expressed as a quadratic drag law in the form

$$F_{farm} = \rho C_F A_C |u| u \tag{1}$$

where u is the free-stream velocity and C_F is the farm drag coefficient based on the channel's cross-sectional area A_C. C_F aggregates the effect of the drag due to power extraction by individual turbines, as opposed to C_D which is typically used for the drag coefficient of the natural background bottom friction. In channels with complex bathymetry the free-stream flow may differ for each turbine, however to keep the discussion here simple, all turbines will be assumed to experience the same free-stream flow and have the same drag coefficient. Conceptually for this simple farm of identical turbines, the farm's drag coefficient can be split into two parts, one due to support structure drag and another due to power extraction

$$C_F = \frac{N}{2A_C}(A_S C_S + A_T C_{T1}) \tag{2}$$

where N is the total number of turbines in the array. C_{T1} is one turbine's "thrust" coefficient based on the area swept by the blades A_T. C_S is the gross drag coefficient of the structure supporting one turbine, e.g. any tower, fairing, and mooring lines, based on their frontal area A_S [18]. Thus the force on one turbine and the power produced by one turbine in an array can be expressed as

$$F_1 = \frac{\rho}{2}(A_S C_S + A_T C_{T1})|u|u, \quad P_1 = \frac{\rho}{2} C_{P1} A_T |u|^3 \tag{3}$$

where C_{T1} is the thrust coefficient of a single turbine and C_{P1} is its power coefficient. For an isolated Betz turbine the optimal coefficients are $C_{T1}^{betz} = 8/9$ and $C_{P1}^{betz} = 16/27$ [47,48]. For a cross-channel row of M turbines it is also useful to define the channel blockage ratio $\epsilon_B = A_T M / A_C$, as a measure of how much of the channel's cross-section is occupied by the turbines. Viewing Eqs. (1)–(3) in terms of the competing effects on an array: "channel-scale dynamics" reduces the free-stream velocity u, while the "duct-effect" enhances the turbine thrust coefficient C_{T1} and power coefficient C_{P1} as ϵ_B increases. As a result of this competition, increasing ϵ_B may or may not result in additional power from the turbine, depending on the relative importance of the two effects.

Models for turbines within a coastal model fall between two extreme types, those which tune by manipulating the aggregated drag coefficient of the farm C_F and those which tune by manipulating the drag coefficient of the individual turbine C_{T1}. The most basic approximation for modeling power extraction is to enhance the natural bottom drag coefficient by C_F over the area spanned by the array, a "distributed-drag" approach. GC05 is an example of this first extreme, where the farm was modeled as a single drag coefficient in a 1D channel which can be adjusted to find the channel's maximum power output, i.e. its "potential". This distributed-drag approach has also been used within 2D and 3D numerical models of real channels, e.g. [49,50,46]. Though relatively easy to implement, the distributed-drag approach does not provide a direct way to connect power production to the number of turbines in the array, thus cannot be used to estimate how many turbines are required to realize a given power output. In addition, the distributed-drag approach does not have a parametrization of the sub-array scale turbulence. Thus it does not account for the significant power lost to mixing behind individual turbines and the array as a whole, power which is then not available for electricity production [18]. Thus except when used to estimate a channel's "potential", or that from a tidal fence filling almost all of the cross-section of the channel, array-effect #2, the distributed-drag approach may significantly over estimate array power production.

Some hybrid models have used distributed-drag, in which a fixed C_{T1} value is used to estimate the number of turbines required to match the drag force on the farm (1), e.g. [50] where they used $C_{T1} = 0.8$ and $C_{P1} = 0.45$, as a representative of an isolated turbine. However both the optimal thrust and power coefficients for turbines within an array may be several times larger or smaller than from those of an isolated turbine [8], see Section 4.1. Thus hybrid models may significantly distort estimates of the number of turbines required to produce the power dissipated by a distributed-drag model.

The other extreme approach is to model individual turbines within the coastal model. This approach explicitly resolves turbulence at the sub-turbine scale ($\approx$1 m) but not the blade scale ($\approx$0.1 m). There are several ways to model individual turbines. The simplest way is to use small areas of enhanced drag to mimic power extraction by individual turbines. For these, the free-stream flow in (1) is replaced by the velocity across each turbine and power is summed over all turbines. Though more realistic, the computational cost of modeling scales spanning the size of the coastal domain to sub-turbine scales is still very high. Examples of individual turbines modeled with enhanced drag are given by [42,43]. This approach clearly allows for the power lost to mixing behind individual turbines and the array, but it increases the computational effort required to tune these turbines by a factor equal to the number of turbines or more. A daunting prospect for arrays with hundreds of turbines. One way to reduce this additional effort is to assume that all turbines have the same drag coefficient, i.e. the C_{T1} are all equal [42], or to adopt recent advances which can eliminate most of the additional computational cost of individualized tuning of drag coefficients, see Section 6.

There are several approaches for modeling large arrays which fit between the two extremes of "distributed-drag" and "individual-drag" by modeling the link between the farm's drag coefficient and the thrust coefficients of its turbines. An early example of a "group-drag" approach was [23, hereafter GC07], who extended classic actuator disk theory for an isolated turbine [47,48] to a row of turbines in a 1D channel. V10 took this to the next level by properly

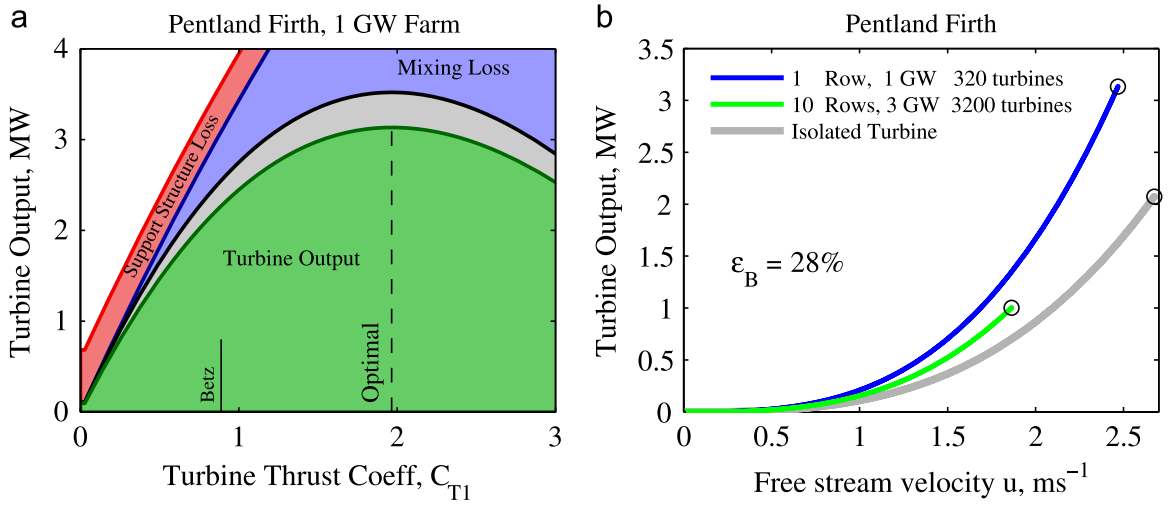

Fig. 5. Turbine performance in arrays. (a) Example of tuning turbines in a single row array of 320 turbines in Pentland Firth. A green curve is the turbine power output. Output peaks at an optimal turbine drag coefficient, which is well above the optimal for a Betz turbine $C_{T1}^{betz} = 8/9$. The green area is the power output of each turbine, the gray area the electro-mechanical losses within the turbine, the blue area is the losses due to turbulent mixing behind the turbines and the red area the losses due to drag on the turbine's support structure. (b) Power curves for optimally tuned 400 m^2 turbines in arrays within the Pentland Firth. Gray curve is a "manufacturer's" power curve for an isolated turbine operating in the velocity along the undisturbed channel. The gray curve is almost the same as the power curve for the first turbine installed in the channel. Black circles show maximum turbine output in the channel accounting for any reduction in the maximum free-stream flow due to power extraction by the array. (For interpretation of the references to color in this figure caption, the reader is referred to the web version of this paper.)

combining the GC07 approach with the channel-scale model of GC05, showing that the optimal tuning given in GC07 for a fixed free-stream flow is sub-optimal in a tidal channel. Houlsby et al. [51] extended GC07's 1D actuator disk in a channel model to allow for free surface effects and the authors of Refs. [45,46,14] embedded lines of Houlsby et al.'s [51] actuator disks in 2D coastal numerical models, in order to simulate rows of turbines. These intermediate approaches are examples of "upscaling" the gross effects of a turbine to form groups of turbines which are more coarsely resolved, eliminating the computational cost of resolving turbine scale turbulence. It would also be possible to "upscale" the drag and wake structure from detailed 3D CFD turbine models or laboratory measurements [52] to more realistically incorporate turbine behaviour within a coarser resolution coastal model, either as individual turbines or in groups. However, this would require many 3D CFD model runs or experimental setups to extend across the range of free-stream flow speeds which could exist within the coastal model and the range of turbine blockage ratios which are being explored with the coastal model.

4. Macro-arrangement of arrays: *review*

Understanding why compromises in macro-array design given in Fig. 3 occur, requires an understanding of aspects of the dynamics of turbines within arrays. This section outlines how the turbines perform in arrays of different arrangements, how adding turbines to a row differs from adding the same number of turbines as new rows. It also reviews how turbine numbers and arrangement affect the loads on the turbines, which in turn affect turbine construction costs.

4.1. Performance of turbines within large arrays

Before discussing turbine arrangement it is important to understand how the array affects turbine performance, in particular turbine power output, V10. All turbines require tuning to maximize their output. This is typically done by adjusting blade pitch. Fig. 5a illustrates the tuning of turbines for an array in the Pentland Firth by plotting turbine output against the thrust coefficient of a single turbine, C_{T1} (2). Fig. 5 shows that the power production of a turbine in the array peaks at values which differ in the two example channels and is higher than the optimal thrust coefficient of an isolated turbine $C_{T1}^{betz} = 8/9$. This illustrates the array and channel specific turbine tuning required to maximize turbine performance V10, array-effect #3. Fig. 5 also shows that the flow is losing much more power than the power output of the turbine. Almost as much power is lost to mixing due to turbulence behind the turbines. For a Betz turbine, 1/3 of the energy lost by the flow is lost to mixing behind the turbine [53]. For arrays of tidal turbines the fraction lost to mixing varies from 1/3 to almost zero at high channel blockage ratios [18]. In addition another 5–10% is lost to drag on the support structure, along with the assumed 11% to electro-mechanical losses [26]. The forces associated with these additional losses make up a large fraction of the load on a turbine, thus it is important to understand their contribution in order to develop structural design specifications. The proportions of these losses vary with turbine number, tuning and arrangement.

The conventional approach for assessing turbine performance is to compare the turbine's power coefficient to the Betz limit of $C_{P1}^{betz} = 16/27$ [47,48]. This approach is not appropriate for turbines within large arrays. Firstly, because the duct-effect can allow the power coefficient to exceed the Betz limit, [GC07, 8]. Secondly, power extraction reduces free-stream velocity u in (3), which limits the maximum output of the turbine. A more useful measure of turbine performance is comparing turbine power output (3) to the power output of an isolated turbine which is operating in the free-stream flow in the channel without any turbines [8]. The comparison of turbine output performance with an isolated turbine is almost the same as a comparison with the performance of the first turbine installed in the channel.

Fig. 5b demonstrates that the power coefficients of the turbines in the Pentland Firth can exceed that of an isolated turbine given by the gray curve [8]. The gray curve gives the power versus velocity performance curve of an isolated turbine operating in the undisturbed free-stream flow. It has a power coefficient of $0.89 \times 16/27$, i.e. a turbine at the Betz limit with an assumed 89% power train efficiency. The optimal power coefficient for turbines in the Firth examples significantly exceeds that of an

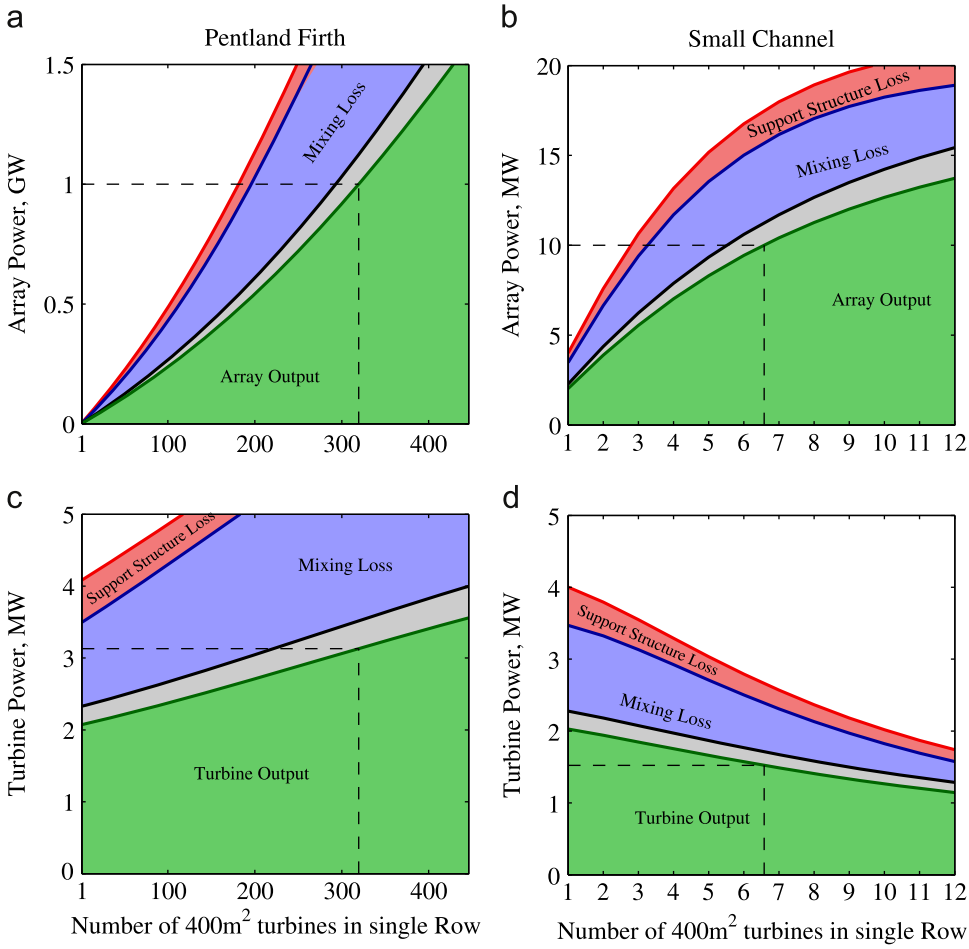

Fig. 6. Effect of expanding an array with a single row in the two example channels. Line and area colors as used in Fig. 5a. (a) and (b) A green curve is array output at peak flow in GW. (c) and (d) A green curve is power output of each optimally tuned turbine at peak flow in MW. Dashed lines highlight 1 GW or 10 MW arrays. (For interpretation of the references to color in this figure caption, the reader is referred to the web version of this paper.)

isolated turbine, with the maximum turbine output in the one row array also exceeding that of an isolated turbine. However, a high power coefficient does not necessarily mean higher turbine output, as shown by the 10 row array where power extraction reduces the maximum free-stream flow well below that experienced by the first turbine installed in the channel. Flow reduction also means that the 10 row array produces only 3 times the total output of the 1 row farm, despite having 10 times the number of turbines. For the small channel (not shown) turbine power curves for multi-row arrays lie below the curve of an isolated turbine.

4.2. *Effects of adding turbines to a row*

Fig. 6a–d gives the array and turbine power outputs for a single row of optimally tuned turbines in the two example channels, all of which display significant array-effects. The figure is essentially a vertical slice along the left hand side of the contour plots in Fig. 2. Fig. 6c and d clearly illustrates array-effects #5 and #6, where for the Pentland Firth, adding turbines to a row increases every turbine's output, while in the small channel, adding turbines to a row decreases the output of all turbines which affects both loads and array construction cost, array-effect #7.

The mixing and support structure losses are substantial in Fig. 6, amounting to typically around half the total energy lost by the flow. The forces associated with these losses, along with the drag forces due to power extraction, contribute to the total load on the turbines. The load forces (not shown) follow the trends in the power output per turbine, increasing in the Firth and decreasing in the small channel, as turbines fill the cross-section.

For a single row in the Firth, 40 turbines are a large array of turbines, i.e only $\epsilon_B = 3\%$. For a single row it takes just 320 turbines in the Firth to produce 1 GW, because the duct-effect has boosted each turbine's output from 2 MW to 3.1 MW, Fig. 6c. In the small channel one 400 m^2 turbine blocks 4% of the cross-section and all arrays are "large" and 7 turbines in a single row are required to produce 10 MW. This is because a 20% flow reduction has reduced turbine output from 2.0 MW to 1.4 MW, Fig. 8b.

4.3. *Effects of adding rows of turbines*

Fig. 7 illustrates several array-effects due to adding rows. The figure is essentially three horizontal slices through the contour plots in Fig. 2. In both examples adding rows increases array output, but decreases the output of each turbine, array effect #6. If the rows added to the array have the same number of turbines, then all rows have the same channel blockage ratio. As the duct-effect remains unchanged, the power per turbine falls as rows are added because of the free-stream flow reduction due to channel-scale dynamics, Fig. 8a and b. Thus in all regular grid arrays, adding rows with the same or smaller blockage ratio results in a diminishing return on the additional turbines. Turbine loads (not shown) show the same downward trend as the power per turbine. The diminishing power return is harsh in the small channel for

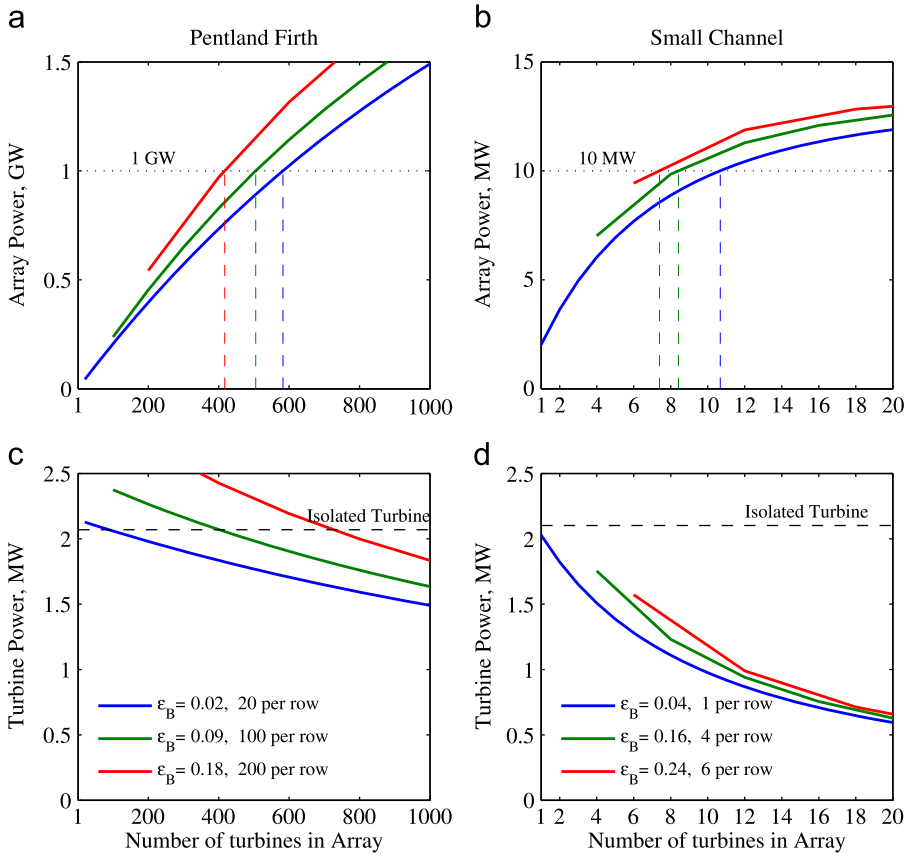

Fig. 7. Effects of expanding an array by adding rows of turbines. Colored lines correspond to a different number of turbines per row, or blockage ratio, as given in the legend. In upper two plots (a) and (b) the vertical dashed lines highlight the number of turbines in 1 GW or 10 MW arrays for each blockage ratio. In lower two plots (c) and (d) the horizontal dashed line shows output of an isolated turbine operating in the undisturbed flow. (For interpretation of the references to color in this figure caption, the reader is referred to the web version of this paper.)

arrays of more than 6 rows, as the output is near the maximum possible in the channel after mixing, support and electro-mechanical losses. Thus extracting 10 MW at peak flow from the small channel is challenging despite a 21 MW potential at peak flow.

4.4. Loads on turbines and the effect on construction costs

Fig. 8c and d show the maximum force on the turbines due to power extraction and support structure drag. These forces are spread across the turbines blades and their support structure, as well as the turbine's mooring system and power train. However, Fig. 8c and d are indicative of the relative forces on these components for different array designs. Higher loads will require stronger, more robust, turbines which will be more expensive to manufacture. Adding turbines to a row for moderately-large arrays in the blue area boosts individual turbine output, but makes all turbines in the array more expensive to manufacture. Thus, in addition to a compromise between array output and navigation, there is also a compromise between power output per turbine and structural loads when adding turbines to the rows for arrays in the blue area. As a result, not only is the number of turbines in a row limited by the need to maintain navigation, it may also be limited by the cost and feasibility of building the turbines to withstand additional loads [8]. However, for arrays outside the blue area, the upside of a diminishing return on turbines added to the row or additional rows, is that the loads on the turbines reduce. Thus less robust cheaper turbines could be used in these “very-large” arrays, mitigating the poorer returns on additional turbines. The edge of the blue area which marks the boundary between moderately-large and very-large arrays, has turbines which produce the same output as an isolated turbine and have similar loads. Thus, for arrays which add turbines in a way that follows this boundary, turbine loads and output remain similar to those for the first turbine installed in the channel.

4.5. Assessing array performance, farm-efficiency

One approach to assessing array performance, as opposed to turbine performance, is “farm-efficiency”. Farm-efficiency can be defined as the fraction of a channel's potential that a farm is able to output [10] and therefore is a useful measure of how effective the farm is in realizing a site's potential Fig. 8e and f. The small example channel is so small that array layouts in Fig. 2b can extend to extremely-large arrays in the gray area of the upper right. Here, adding turbines reduces the array's efficiency. Clearly extremely-large arrays are not economically viable. The small channel example also illustrates that, for all channels where maintaining navigation restricts the number of turbines in a row, the maximum array output is well below the channel's potential. In other words, restricting the maximum allowable channel blockage means that the maximum farm-efficiency is well below 100%. Going further, the widening gaps between the farm-efficiency contours in Fig. 8e and f at higher efficiencies indicates more turbines are required to increase the power output by the same amount. This harsh diminishing return on new turbines means farms in both examples are unlikely to exceed 60% efficiency.

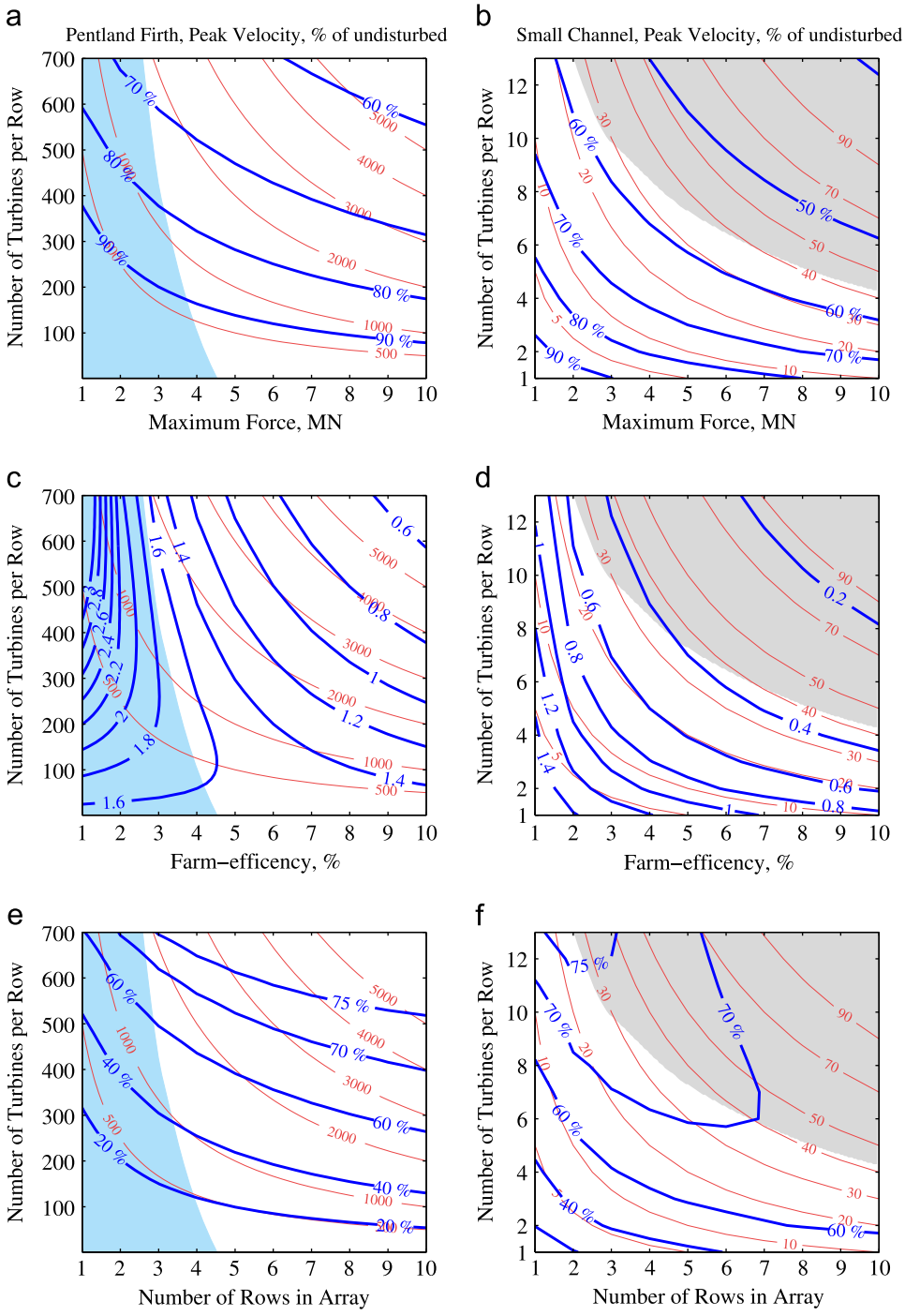

Fig. 8. Other design parameters for large arrays of optimally tuned tidal turbines in the two example channels at peak flow. Faint red contours show the number of 400 m^2 turbines in the array. Top row is the free-stream velocity as a percentage of the undisturbed flow. The middle row is maximum force due to the combined effects of power production, mixing and support structure drag. The lower row is farm-efficiency, the array output as a percentage of the channel's potential. Colored regions as in Fig. 2. (For interpretation of the references to color in this figure caption, the reader is referred to the web version of this paper.)

5. Micro-arrangement of turbines within large and small arrays: *review*

Adjusting the relative positions of turbines within regular grids can be used to boost array output in both large and small arrays within channels or at non-channel sites such as at headlands. Placing the turbines downstream of the gaps between turbines in an upstream row can boost output, as can packing turbines to one side of the channel. There may be other micro-arrangement strategies yet to be discovered. Firstly though, an important decision is, how far downstream of a row to place the next row of turbines?

5.1. *Inter-row spacing*

The reduced flow in a turbine wake extends some distance down stream, reducing the “free-stream” flow experienced by the next row of turbines. While tidal turbines may occupy a large fraction of the water depth, wind turbines have kilometers of high speed air moving above them. Thus the distance required for flow to recover behind a

tidal turbine will be longer than that for wind turbines when the recovery distance is measured in blade diameters [54]. The recovery of high flows in wakes behind turbines has been studied with models and experiments. The authors in Ref. [55,34] assumed that wake recovery behind an upstream turbine was the dominant process determining the minimum inter-row spacing and found little benefit to spacing rows of turbines more than 5 diameters downstream. However, this study only simulated 2 turbines, one directly downstream of the other in a channel that was 14 turbine diameters wide. More recently, Malki et al. [56] used blade element theory CFD to examine wake recovery and turbine performance for three micro-arrangements with up to 14 turbines. They demonstrated that recovery takes more than 40 turbine diameters, depending on the arrangement. They also showed that a cross-stream spacing between turbines of less than 3 diameters significantly reduced the output of the downstream turbines.

Bahaj and Myers [52] used experimental and numerical models to characterize the near and far field turbulent wake behind a turbine. Turbulence generated by a turbine may also impact directly on those downstream, as does ambient turbulence in the channel. The effect of ambient turbulence on the inter-row spacing was explored by Harrison et al. [30]. They used a blade element momentum method coupled with a Reynolds-Averaged Navier–Stokes solver and found that increased ambient turbulence decreases the distance required for wake recovery. Experimental and numerical work by Mycek et al. [57] showed that a down-stream turbine is deeply affected by the turbulence and velocity deficit due to an upstream turbine. Hence, an increase in ambient turbulence decreases the inter-row spacing needed between turbines to allow for wake recovery. Mycek et al. [57] used a single turbine per row with periodic across stream boundaries to simulate an infinitely wide array with a channel blockage of 0.3 with fixed free-stream flow. Their model's blockage would easily qualify as a large array (Section 2.6), thus needs a channel-scale model to allow for reduction in free-stream flow. However, the trend of smaller inter-row spacing at higher ambient turbulence is still likely to hold, even if ambient turbulence reduces as free-stream flows reduce. Thus there may be a compromise between a higher inter-row spacing to minimize the power lost due to down-stream turbines experiencing weaker flows and a smaller inter-row spacing which maximizes the number of turbines which can be installed within an allowable area with the channel [57]. There is still much to learn about inter-row spacing in optimizing array layout.

5.2. Staggering rows

Turnock et al. [20] used a Reynolds-Averaged Navier–Stokes model combined with blade element theory to demonstrate that placing turbines downstream of the gaps between turbines in an upstream row can increase turbine output when compared to an unstaggered grid. An increase required inter-row spacings of less than 6 turbine diameters and gaps smaller than 6 turbine diameters. The maximum demonstrated increase of around 20% required an inter-row spacing of only 2 turbine diameters and gaps in the upstream row of 2 turbine diameters. This increased output takes advantage of the enhanced flows through the gaps between turbines due to a localized duct-effect. Their model had fixed stream flow, though their channel blockages were large enough to make the array very significant in channel-scale dynamics. Despite this, power enhancement due to staggered rows has also been demonstrated in a 2D Navier–Stokes model of an array which allows for free-stream flow reduction [42,17]. Lee et al. [34] used a 3D model of 8 turbines and periodic boundary conditions to quantify the effect of inter-row spacing on staggered grids of fixed rotor turbines. They found a row spacing of around 3 turbine diameters was most appropriate. CFD modeling by Malki et al. [56] showed that a cross-stream spacing of more than 2 turbine diameters allows the downstream turbine to benefit from the acceleration of the flow through the gaps. They also showed that for cross-stream spacings less than 2 diameters, the performance of the downstream turbines was significantly compromised for a staggered row more than 2 turbine diameters downstream of the gaps in the first row. Over all they found that optimizing the inter-row and cross-stream turbine spacings could increase array output by more than 10%

Churchfield et al. [31] used a 3D model of turbines represented as rotating actuator lines and also found that staggering consecutive rows of turbines increases turbine efficiency at low inter-row spacings. However, using counter-rotating turbines in consecutive rows in a non-staggered array also produced a small benefit. Again their model used a high enough channel blockage to be a large array, but the trends they observed would still likely occur if channel-scale dynamics were included.

An equally important question concerns how to optimize an arrangement of a given number of turbines. Specifically, should they be packed in to a single row so as to exploit the “duct-effect” or staggered across multiple rows to exploit enhanced flow between gaps? [21] has recently explored this question analytically, extending on the actuator disc models of [23,51]. In the case where turbines all have the same properties, this study suggests that it is not apparent that staggering turbines is a better arrangement than placing all turbines in one row, however staggering is clearly better than adopting multiple rows of non-staggered (i.e. centred) turbines. However, given that the approach in [21] was analytical and it relied on assumptions about the downstream spacing between turbines, further numerical analysis is required to better understand the trade-offs between different arrangements of turbines.

5.3. Packing turbines within rows

The 1D model used here assumes that the turbines are uniformly spaced across the channel. Packing them closer to one side would provide a larger navigable route along the channel and increase power production by up to 15% [19]. The 1D model in [19] exploits a two scale inviscid flow approach to modeling an array, with a turbine scale model embedded within a larger array scale 1D model. This allowed modeling uniformly spaced turbines in a row which only extends part way across the channel. The optimal inter-turbine spacing within the packed row depends on what fraction of the channel's cross-section the turbines occupy. Viewed another way the two scale approach of [19] for an array protruding from one side of a wide channel demonstrates that a “shoreline-effect” can be used to boost output if the inter-turbine spacing is optimized. The shoreline-effect exploits the difference between mixing on the turbine scale and mixing which occurs around the array as a whole. The two scale approach was improved in [16] and is shown to compare well with a 3D Reynolds-Averaged Navier–Stokes model of up to 40 actuator disk turbines.

The [19] approach assumes a fixed free-stream flow and therefore is limited to small arrays. [19] used an example with $\epsilon_B = 30\%$ which would significantly exceed the criteria to be a large array, while [16] used much smaller global blockages of $\epsilon_B = 0.1\%$, which easily meets the criteria to be a small array. To properly quantify the benefits of packing turbines within a row of the large arrays required to realize much of a channel's potential the [19] approach needs to be embedded within a channel-scale model. However, their approach still demonstrates that there is a significant benefit from optimizing the inter-turbine spacings.

The benefits of staggering turbines in adjacent rows and packing turbines within rows are not independent. Staggering turbines exploits the enhanced flow though gaps in the upstream

row, which will be affected by the size of these gaps which are optimized to pack turbines within a row. In the extreme cases of very small or large gaps, staggering will likely have little additional benefit. Thus there needs to be further modeling and experimental work to explore the interaction between optimizing the size of the gaps and how a second row of turbines is staggered relative to the upstream row in order to maximize array output.

6. The future?

6.1. Combined macro- and micro-arrangement?

To date, array design has focused on grids of turbines with identical power coefficients. However, real channels have complex geometries and flow patterns, and the optimal turbine arrangement is unlikely to be a grid of turbines each with the same power coefficient. Instead, turbines will differ in their output depending on where they are positioned in the channel and hence will require individually tuned power coefficients [10].

Individualized tuning comes at a high computational cost as many model runs are required to search for the set of tunings which maximizes the array output. By using optimization algorithms that incorporate gradient information, i.e. the sensitivity of the power production to the turbine tunings, the required number of model runs can be significantly reduced compared to algorithms which only incorporate the array power, e.g. [58,59]. Such gradient-based algorithms use the gradient vector to iteratively change an initial set of tunings to best increase the farm's output, moving one step closer to the optimal set of tunings. However, computing the gradient of the total power production with respect to the turbine tuning parameters comes at a very high computational cost itself, if the model can only calculate the power for a given set of turbine tunings. In this case, estimating the gradient vector for N turbines would require N additional model runs at each optimization step, making it prohibitive for 2D and 3D hydrodynamic models.

An exciting recent development by [43, hereafter FFP14] is the application of adjoint methods to optimize tidal turbine farms using a 2D shallow water hydrodynamical model with an unstructured grid, where individual turbines are modeled as areas of enhanced bottom drag. Adjoint methods yield the gradient vector of the farm's power with respect to changes in the turbine tuning by numerically solving one related “adjoint” model. This reduces the computational cost for computing the gradient by a factor of N and results in a total cost for optimizing the turbine tunings which is almost independent of the number of turbines. In addition, the gradient calculation can be extended for use in optimizing the positions of the turbines within the array as part of the same adjoint model. Remarkably, FFP14 were able to optimize both the tunings and positions of 256 turbines in less than 200 forward model and adjoint model runs.

Fig. 9 illustrates the application of adjoint optimization to a small array of 50 turbines in the southeastern Pentland Firth (see FFP14 for details of the model). In the complex flows around the island of Stroma, optimization has distorted the initial grid of turbines into arcs of turbines with an array output 14% higher than that of the initial grid. In the initial grid the upstream row reduces flows for downstream rows. In the optimized array, high flows extend further downstream and power output appears more evenly distributed across the array. Blockage by both the initial and optimized array has diverted flow around the array, resulting in higher flows on the south side of Stroma than in the undisturbed channel.

Fig. 10 gives examples of adjoint optimized arrays in the small channel example introduced in Section 2.3. The example is extended to include a headland, which restricts the channel width and provides an interesting illustration of the effects of alternating tidal flow directions on array design. The turbine positions were optimized to maximize the total power output from the ebb and flood tides This optimization produced symmetric array designs, despite flow patterns around the headland being asymmetric during the ebb and the flood tides. For arrays of up to 16 turbines, the optimal arrangement was a single row of turbines in the narrowest cross-section of the channel (Fig. 10a). In the 16 turbine example, three turbines around the headland and two in the reduced flow near the other side of the channel produce little power, thus 11 turbines produce most of the power. However, these low producing turbines boost array output by 10% above that of an optimized 11 turbine array (Fig. 10c). For 20 or more turbines the optimal arrangement is two rows of turbines (Fig. 10b). Thus the optimal adjoint designed arrays in the 2D model support the 1D results of V10 and [10], which noted that the highest array output is obtained by putting as many turbines as possible in one row before adding another row. It is also interesting that the optimized turbine locations are not staggered turbines, which tends to support [21] in that more power is extracted from the same number of turbines in a single row than that number in a pair of staggered rows.

Though FFP14's 2D model is clearly more realistic than the 1D models of V10 used in most of this review, the estimated array output and power per turbine from the two models are remarkably similar despite the very different modeling approaches, Fig. 10c and d. The 2D model array output exhibits a diminishing return on new turbines, i.e. falling output per turbine as the array grows, as predicted for small channels by 1D models, Fig. 7d. The output per turbine for small arrays in Fig. 10d is well above the maximum of around 1 MW for the largest operating turbine [26]. This is a result of the 2.7 m/s flows across the ends of the small channel, Table 1, being accelerated to 3.7 m/s in the narrowest cross-section of the undisturbed channel. No existing turbine could withstand the loads at these high flows. However, the flow experienced by turbines in arrays with two rows is reduced by turbine placements outside the narrowest cross-section, along with power extraction significantly reducing flows throughout most of the channel to less than 2 m/s, a point where turbine outputs are within the range of existing turbines.

While adjoint methods can significantly reduce the number of model runs required to optimize turbine tuning they are much more complex to implement. Also, a straight-forward implementation of the adjoint approach results in much higher computer storage requirements as they require that the velocity and surface elevation from the “forward” hydrodynamical model for an entire tidal cycle be stored for use by the adjoint model, although there are techniques to reduce computer storage requirements, FFP14. The adjoint optimization can also be “trapped” within local maxima and so it may need to be started from many different initial turbine positions in order to find the global maxima. However, the advantage is that the adjoint approach essentially combines macro-arrangement and micro-arrangement in a unified approach to array design optimization which is not restricted to grids of turbines. The ability to optimize turbine positions also adds an additional feedback, where the channel-scale dynamic effect is now coupled with changes to the underlying flow patterns within the channel due to the turbines.

The adjoint approach can also be used to impose practical and engineering constraints, such as where turbines can be located, or maximum allowable turbine loads, or to include economic factors. Though there is still a long way to go to realize the potential of adjoint methods to integrate macro- and micro-design, they are an exciting approach which can make individually optimizing the tuning and position of turbines within an array computationally tractable.

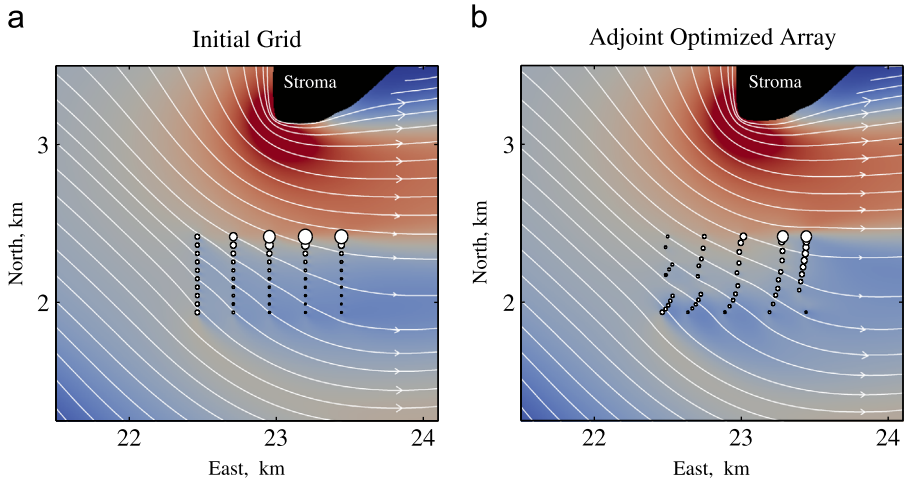

Fig. 9. Example of designing a 50 turbine array using adjoint methods in the south eastern Pentland Firth between the Island of Stroma and mainland Scotland. (a) Initial grid of turbines. (b) Turbine positions and drag coefficients optimized using adjoint methods after 120 iterations. Size of turbines indicatives relative power production. Turbine locations were constrained to lie within a rectangle (Section 6). White lines are streamlines of the flow. Colors indicate flow speed, dark red is 5 m/s and dark blue near 0 m/s. See [67] for animation of optimization steps of similar examples. (For interpretation of the references to color in this figure caption, the reader is referred to the web version of this paper.)

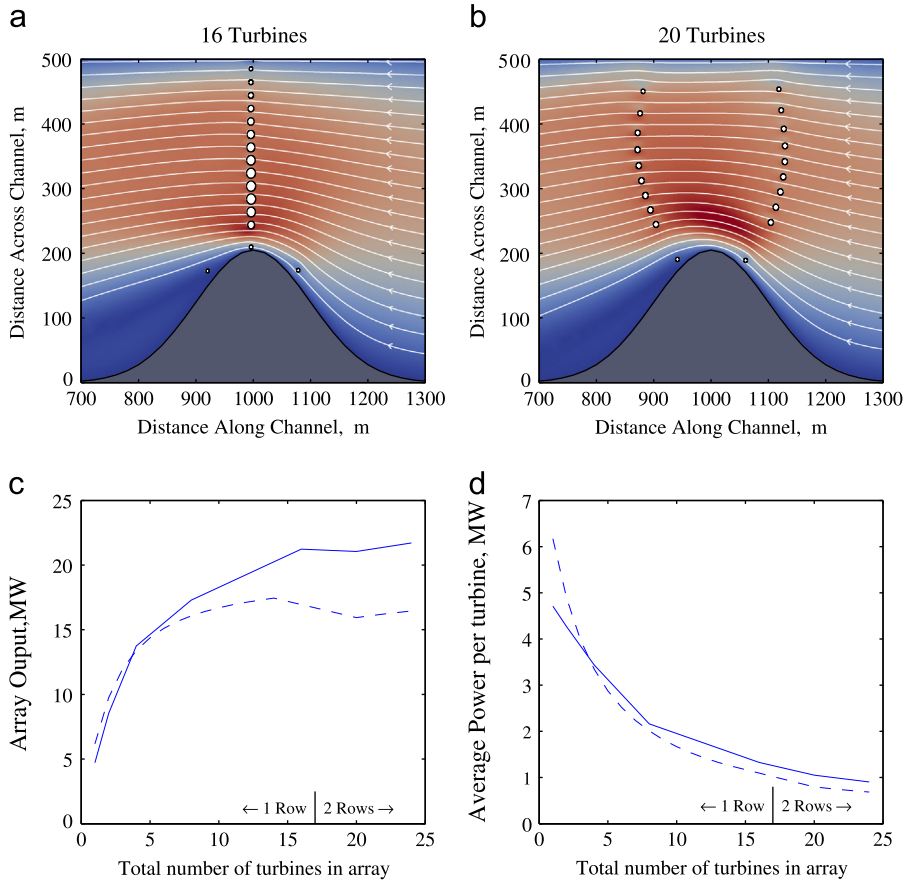

Fig. 10. Arrays in the small channel example with a headland constriction designed by combining adjoint methods with a 2D hydrodynamic model. Headland in a 2 km long, 500 m wide, 20 m deep channel reduces channel width by 40%. See [43] for details of model implementation. (a) Optimized 16 turbine array. White dots give turbine locations and the area indicates their relative power production. Flow in example is from right to left. Colors indicate flow speed, dark red is 2 m/s and dark blue near 0 m/s. (b) Optimized 20 turbine array. (c) Array power output for different optimized array sizes. For small array one row is optimal, for larger arrays two rows are optimal. Dashed line shows output from optimized actuator disk arrays in 1D model with a constriction [18], and with the same number of rows as adjoint optimized arrays in 2D model. (d) Average power output per turbines for optimized arrays (Section 6). (For interpretation of the references to color in this figure caption, the reader is referred to the web version of this paper.)

6.2. ∗ *A turbine economic efficiency index?*

For both macro- and micro-arrangements of turbines there is a trade off between the output of a turbine and the loads on the turbine, which increases construction costs. A simple way to quantify this 3↔4 trade off is a Turbine Economic Efficiency Index (TEEI), given by the income from a turbine's power output divided by the cost to build the turbine. Quantifying the construction costs

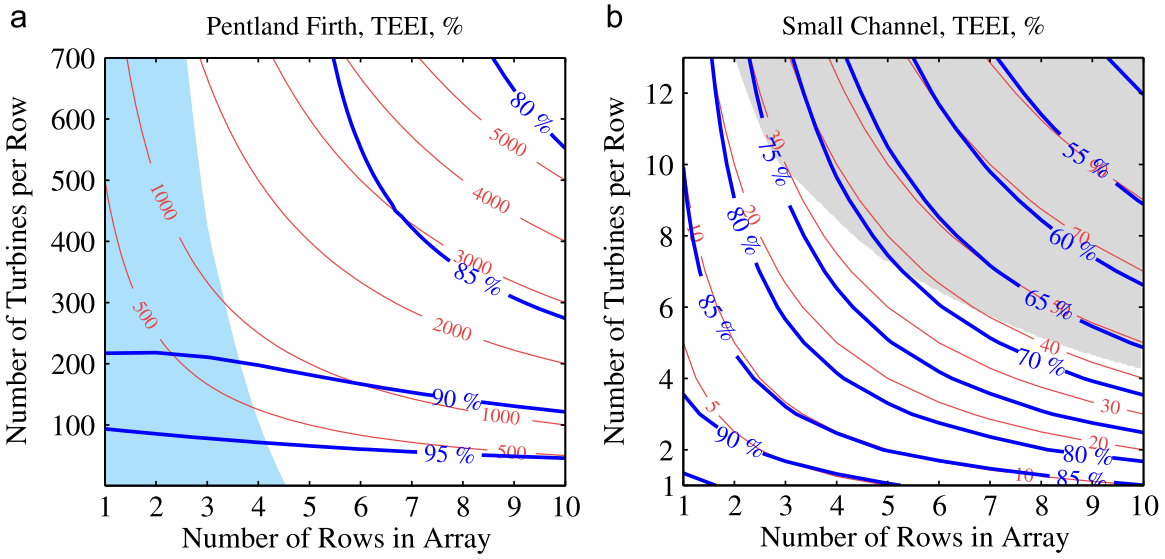

Fig. 11. Turbine Economic Efficiency Index relative to the TEEI of an isolated turbine in the undisturbed flow for the two example channels in Fig. 2. The TEEI is a benefit to cost ratio for turbines in arrays as measured by the turbine's power output to load ratio (4). Colored regions, red contours and gray lines as in Fig. 8. (For interpretation of the references to color in this figure caption, the reader is referred to the web version of this paper.)

of a turbine is complex. However, here we are interested in the relative cost to build a turbine with the same external dimensions, i.e. area swept by the blades, height and external diameter of any supporting tower, thickness of the blades etc., for different loads associated with a higher or lower power output per turbine. If the maximum permitted stresses within the structure are the same under all loads, then for fixed external turbine dimensions the wall thicknesses of the components must increase in direct proportion with the load. Thus the weight of the material required to build a turbine is proportional to the load for fixed external dimensions. A tested wind turbine costing approach, Equation 9.3.2 in [60], has the cost of individual subsystems being proportional to their weight, times calibration and complexity factors. Here the external size and design of the components remains the same, thus the complexity factors will likely remain the same. Consequently, it may be argued that total tidal turbine cost will be roughly proportional to the total turbine weight. For fixed external dimensions weight is proportional to the applied load, thus construction costs will roughly depend on turbine load in a linear fashion. Adopting this idea, a new concept is the TEEI, or turbine benefit to cost ratio for turbines of the same physical size, which is equal to the power output-to-load ratio

$$TEEI = \frac{k_P P_1}{k_c F_1} = \frac{k_P C_{P1} |u|}{k_c (C_{T1} + A_S C_S / A_T)} \tag{4}$$

where P_1 is the power output of one turbine and k_P is the dollar income per Watt of turbine output. F_1 is the load on one turbine due to power extraction and support structure drag and k_c is the dollar cost to build a fixed size turbine to withstand each Newton of load. Determining values for k_P or k_c is difficult, but here we give the TEEI for a turbine in an array relative to that of a single isolated turbine operating in the undisturbed free-stream flow. This relative TEEI index assumes that the isolated turbine and the turbines in the array benefit equally from the economies of scale of producing a large number of turbines at the same time. The TEEI uses the total load on the turbine, whereas turbine components will experience different loads. Thus the index should only be viewed as an indicative turbine benefit-to-cost ratio, one which is broadly useful in comparing the economics of turbines in different arrangements.

Fig. 11 gives the relative TEEI for turbines in large simple grid arrays in the two example channels. This gives a new and very different picture of designing large arrays. For both examples, the TEEI is always less than that of an isolated turbine, suggesting that the economics of building turbines in an array is always worse than that of an isolated turbine. In the Pentland Firth, the variation in TEEI is remarkably small given the large variation in turbine output and loads in Figs. 2a and 8a, varying by only 20% in the example arrays. Fig. 2 shows that for both examples putting as many turbines into a single row first then adding rows of turbines to increase array output appears to give the most economical array, because this yields the highest power output per turbine. However, the TEEI for the Firth Fig. 11a demonstrates that this is outweighed by the additional cost to build those turbines to withstand higher loads. Thus contrary to previous works [11,18,8], for larger channels like the Firth the most economical arrangement may be to place one turbine in many rows first, then add turbines to each row to increase array output.

For the small channel, Fig. 11b, TEEI has a larger variation and TEEI contours are almost parallel to contours of the number of turbines. Thus, in the small channel turbine economics is almost unaffected by how a given number of turbines are arranged into rows. However for smaller arrays in the small channel there is a slight gain in TEEI by having a few turbines in many rows, but for larger arrays there is a slight advantage in placing as many turbines as possible in one row before adding rows. However, the TEEI is only a basic measure of array economics and there is still much to learn, for example the effects of the costs of cabling and power conversion equipment on array design.

7. Discussion

The 1D channel model discussed here makes it computationally possible to optimize the 100 s of arrays in different channels needed to give an overview of array design. There is also remarkable agreement between the 1D and 2D models for the idealized small channel example, Fig. 10c and d. However, real channels have complex geometries, irregular shorelines, curved axes, headlands, depth variation both along and across the channel, or islands which split the channel. The 1D model also ignores any effects on down-stream rows due to wake recovery or turbulence. To better quantify the power extraction by arrays will require computationally expensive 2D and 3D models. Depth averaged 2D models do not allow for the reduction of the velocity near the sea

bed depth due to bottom friction. This reduction means that depth averaged models do not allow for variations in output due to the height of the turbine's rotational axis above the sea bed [32]. In addition, depth averaged models may not account for the flow which bypasses above or below the turbine. Also, shallow water 2D numerical models do not properly model 3D turbulence [61], thus they may also not properly account for turbulence behind the turbines and dissipation of energy from the flow. Nor do 2D models capture secondary flows in curved tidal flows [62], which may impact on the flow speeds and directions experienced by turbines at different heights above the seabed, at headlands or in curved channels. 3D models are needed to improve on depth averaged 1D and 2D models. This would come at a high computational cost, but the 3D effects of turbines could be "upscaled" within coarser 3D coastal models.

A 1D model of a simple channel connecting two large water bodies is used here to discuss the design of large arrays. The results could be extended to many other geometries, such as a channel connecting an ocean to a large lagoon which can store water [63], or a channel split into two by an island [64]. They could also be extended to channel networks [65,66] or arrays in the open ocean [15]. Space limitations prevent further discussion of this, however there will be other design issues and compromises relating to these other geometries which must be understood to develop these types of sites.

7.1. Environmental and other constraints on array design?

There are many environmental and practical constraints on array design beyond the possible effects of free-stream flow reduction noted above. For example, the presence of marine mammals or a particular fishery may preclude turbines in some areas. Changes in concentrations of faecal bacteria, some of which are transported with sediments may be important [13]. In addition, putting an upper limit on the channel blockage ratio may not be sufficient to maintain navigation past the array. For example, structures, shipping corridors and channels may limit where turbines can be located. The location of a connection to the electrical grid, or the length of underwater cabling, may constrain an array's location or design. The simple grid arrays that maximize power output, which are the focus of much research to date, may be distorted by practical limits on water depth or steep seafloor topography. In addition, flow reduction downstream of headlands, or at the sides of a channel, may create low flow zones downstream which are uneconomic to use, as in Fig. 10. The length of the channel may also limit how many rows can be installed with sufficient spacing to allow for wake recovery, Section 5.1. Thus designing arrays for real sites is much more complex than that covered by much research to date. However, the adjoint approach to optimizing array layout in real channels in Section 6.1 could be extended to include many of these practical or economic constraints.

8. Summary

Large arrays of tidal turbines must be built in order to realize the global potential of tidal current energy. This potential mostly resides in the concentrated flows along tidal channels. Before large arrays are built, those assessing the tidal current resource available from a channel site must grapple with the compromises inherent in designing large arrays in order to estimate the costs of building an array and the income it could produce. For large arrays there is no simple relationship between the total installed capacity of the turbines in the array and the array's total power output, because the power output of an individual turbine strongly depends on array design. Essentially, there is no simple relationship between the total cost of the turbines, or the loads on them, and the income from the array's total power output, because cost and income are affected in very different ways by the dynamics of the channel, the size of the array and its arrangement. These last two parameters are also constrained by the need to maintain navigation along the channel and an environmentally acceptable flow, Figs. 2 and 8.

To be a large array, the turbines only need to block 2–5% of a channel's cross-section, Fig. 4. This is just one 400 m^2 turbine in the small channel example, or a row of 40 turbines in the Pentland Firth. Turbines in large arrays must be designed for different conditions than isolated turbines, Section 4.1. Importantly, turbines must be designed for the full sized array, not for the conditions experienced by the first turbine. Turbine and array design is an iterative process, as the designed turbine output affects total array output, which in turn affects the flows experienced by each turbine, the loads on the turbines and their outputs. The way turbines are viewed and the criteria used to design them needs to change as we progress towards developing the large arrays of tidal turbines required to realize the potential of tidal current power.

The beginning of a language to discuss large arrays includes physical concepts such as, a channel's "potential", "farm efficiency", flow reduction due to "channel-scale dynamics", the "duct-effect", "array-effects", the "shoreline-effect", turbine "packing" and "staggering", along with labels such as "large arrays", which are divided into "moderately-large", "very-large" and "extremely-large" arrays. Other labels are "large channel" or "small channel", based on how important background bottom friction is within channel dynamics, and "distributed-drag", "group-drag" and "individual-drag" to differentiate ways of incorporating turbines into hydrodynamic models. The language also includes the economic consequences of the physics, concepts such as "increasing or diminishing power return", "TEEI" and the cost of building turbines to withstand fluid dynamic loads.

The contour plots in Figs. 2 and 8 outline some of the design compromises made in growing an array by adding rows or by adding turbines to the rows. Compromises are between the total power production, the power produced by each turbine, the cost of building the turbines to withstand structural loads, the environmental impacts of flow reduction and the need to maintain navigation along the channel. Each of these compromises operates in a different direction within the contour plots. The schematic Fig. 3 illustrates how the directions of these interdependent compromises are orientated, which differs for moderately-large and very-large arrays. Much more work is needed to quantify the cost of each of these aspects in order to optimize farm production and turbine design for a particular array site.

Understandably, much of the current effort in tidal current power research centers on designing, manufacturing and deploying a single turbine, as a step towards deploying arrays with 10 turbines. Ultimately large arrays of 10–100 s of turbines are needed to make a significant contribution to the demand for renewable power. To maximize the output of turbines in a regular grid array, the turbines must occupy as much of the cross-section as possible before adding additional rows of turbines, Sections 4.2 and 4.3. For both example channels the TEEI (4) indicates that the economics of turbines in arrays in channels is worse than that of an isolated turbine. In the Firth the TEEI also suggests that the higher construction costs required to withstand the higher loads outweigh the benefit of a higher output per turbine, thus having few turbines in many rows may be more cost effective, Fig. 11. For the small channel, how turbines are arranged into rows has only a small impact on TEEI, which falls as new turbines are added. For both large and small arrays, whether there are few or many turbines in a row, they may benefit from being "packed" together at an optimal spacing, Section 5.3 and may also benefit from staggering the cross-stream positions in adjacent rows, Section 5.2. However, in real channels with

complex tidal flow patterns the ideal layout may not be a simple grid, Section 6, though maximizing channel blockage to enhance turbine output does appear to push array layouts towards row like arrangements, Figs. 9 and 10.

Designing large arrays is computationally challenging because of the disparity between the size of the turbine and the size of the coastal region which must be modeled. This is compounded by the necessity to optimize the output of each turbine in-concert with the other turbines in the array. These computational challenges require further advances in the hydrodynamical modeling and optimization of arrays which integrate macro- and micro-design, Section 6. There is still much to learn about how to design the layout of turbines in arrays and the turbines within them, along with computational approaches to modeling arrays, in order to realize the potential of tidal current power.

Acknowledgments

Lara Wilcocks for her editing and assistance in the preparation of some figures. This work was supported by New Zealand Marsden Fund Grant number 12-UO-101. S.W. Funke is supported by a Center of Excellence grant from the Research Council of Norway to the Center for Biomedical Computing at Simula Research Laboratory and the EPSRC Platform Grant EP/L000407/1.

References

[1] Blunden LS, Bahaj AS. Tidal energy resource assessment for tidal stream generators. Proc Inst Mech Eng Part A: J Power Energy 2007;221(10):137–46. http://dx.doi.org/10.1243/09576509JPE332.
[2] Sutherland G, Foreman M, Garrett C. Tidal current energy assessment for Johnstone Strait, Vancouver Island. Proc Inst Mech Eng Part A: J Power Energy 2007;221(2):147–57. http://dx.doi.org/10.1243/09576509JPE338.
[3] Blanchfield J, Garrett C, Wild P, Rowe A. The extractable power from a channel linking a bay to the open ocean. Proc Inst Mech Eng Part A: J Power Energy 2008;222(3):289–97. http://dx.doi.org/10.1243/09576509JPE524.
[4] Black and Veatch Limited. UK tidal current resource & economics, Technical report; June 2011.
[5] Vennell R. Estimating the power potential of tidal currents and the impact of power extraction on flow speeds. Renew Energy 2011;36:3558–65. http://dx.doi.org/10.1016/j.renene.2011.05.011.
[6] Adcock TAA, Draper S, Houlsby GT, Borthwick AGL, Serhadlıoğlu S. The available power from tidal stream turbines in the Pentland Firth. Proc R Soc A: Math, Phys Eng Sci 2013;469(2157). http://dx.doi.org/10.1098/rspa.2013.0072 20130072–20130072.
[7] Garrett C, Cummins P. The power potential of tidal currents in channels. Proc R Soc A 2005;461:2563–72. http://dx.doi.org/10.1098/rspa.2005.1494.
[8] Vennell R. Exceeding the Betz limit with tidal turbines. Renew Energy 2013;55:277–85. http://dx.doi.org/10.1016/j.renene.2012.12.016.
[9] Vennell R. Tuning turbines in a tidal channel. J Fluid Mech 2010;663:253–67. http://dx.doi.org/10.1017/S0022112010003502.
[10] Vennell R. Tuning tidal turbines in-concert to maximise farm efficiency. J Fluid Mech 2011;671:587–604. http://dx.doi.org/10.1017/S0022112010006191.
[11] Vennell R. Realizing the potential of tidal currents and the efficiency of turbine farms in a channel. Renew Energy 2012;47:95–102. http://dx.doi.org/10.1016/j.renene.2012.03.036.
[12] Neill SP, Litt EJ, Couch SJ, Davies AG. The impact of tidal stream turbines on large-scale sediment dynamics. Renew Energy 2009;34(12):2803–12. http://dx.doi.org/10.1016/j.renene.2009.06.015.
[13] Ahmadian R, Falconer R, Bockelmann-Evans B. Far-field modelling of the hydro-environmental impact of tidal stream turbines. Renew Energy 2012;38(1):107–16. http://dx.doi.org/10.1016/j.renene.2011.07.005.
[14] Draper S, Borthwick AGL, Houlsby GT. Energy potential of a tidal fence deployed near a coastal headland. Philos Trans R Soc A: Math Phys Eng Sci 2013;371(1985). http://dx.doi.org/10.1098/rsta.2012.0176 20120176–20120176.
[15] Garrett C, Cummins P. Maximum power from a turbine farm in shallow water. J Fluid Mech 2013;714:634–43. http://dx.doi.org/10.1017/jfm.2012.515.
[16] Nishino T, Willden RHJ. Two-scale dynamics of flow past a partial cross-stream array of tidal turbines. J Fluid Mech 2013;730:220–44. http://dx.doi.org/10.1017/jfm.2013.340.
[17] Divett T. Optimising the design of large tidal energy arrays in channels: layout and turbine tuning for maximum power capture using large eddy simulations with adaptive mesh [Ph.D. thesis]. University of Otago; 2014.
[18] Vennell R. The energetics of large tidal turbine arrays. Renew Energy 2012;48:210–9. http://dx.doi.org/10.1016/j.renene.2012.04.018.
[19] Nishino T, Willden RH. The efficiency of an array of tidal turbines partially blocking a wide channel. J Fluid Mech 2012;708:596. http://dx.doi.org/10.1017/jfm.2012.349.
[20] Turnock S, Phillips A, Banks J, Nicholls-Lee R. Modelling tidal current turbine wakes using a coupled RANS-BEMT approach as a tool for analysing power capture of arrays of turbines. Ocean Eng 2011;38:1300–7. http://dx.doi.org/10.1016/j.oceaneng.2011.05.018.
[21] Draper S, Nishino T. Centred and staggered arrangements of tidal turbines. J Fluid Mech 2014;739:72–93. http://dx.doi.org/10.1017/jfm.2013.593.
[22] Vennell R, Adcock TAA. Energy storage inherent in large tidal turbine farms. Proc R Soc A 2014;470(2013.0580):18. http://dx.doi.org/10.1098/rspa.2013.0580.
[23] Garrett C, Cummins P. The efficiency of a turbine in a tidal channel. J Fluid Mech 2007;588:243–51. http://dx.doi.org/10.1017/S0022112007007781.
[24] Bryden I, Couch S. ME1 Marine energy extraction: tidal resource analysis. Renew Energy 2006;31(2):133–9.
[25] Draper S, Adcock TAA, Borthwick AG, Houlsby GT. Estimate of the extractable Pentland Firth resource. Renew Energy 2014;63:650–7.
[26] Douglas C, Harrison G, Chick J. Life cycle assessment of the Seagen marine current turbine. Proc Inst Mech Eng Part M: J Eng Marit Environ 2008;222(1):1–12. http://dx.doi.org/10.1243/14750902JEME94.
[27] Vennell R. Oscillating barotropic currents along short channels. J Phys Oceanogr 1998;28(8):1561–9 doi:http://dx.doi.org/10.1175/1520-0485(1998)028<1561:OBCASC>2.0.CO;2.
[28] Jo CH, Yim JY, Lee KH, Rho YH. Performance of horizontal axis tidal current turbine by blade configuration. Renew Energy 2012;42:195–206. http://dx.doi.org/10.1016/j.renene.2011.08.017.
[29] Shi W, Wang D, Atla rMAM, SeoK-C. Flow separation impacts on the Hydrodynamic performance analysis of a marine current turbine using CFD. Proc Inst Mech Eng Part A: J Power Energy 2013;227(8)833-46, http://dx.doi.org/10.1177/0957650913499749.
[30] Harrison M, Batten W, Myers L, Bahaj A. Comparison between CFD simulations and experiments for predicting the far wake of horizontal axis tidal turbines. IET Renew Power Gener 2010;4(6):613. http://dx.doi.org/10.1049/iet-rpg.2009.0193.
[31] Churchfield MJ, Li Y, PJM. A large-eddy simulation study of wake propagation and power production in an array of tidal-current turbines. Philos Trans R Soc A: Math, Phys Eng Sci 2013;371(1985):20120421–20120421. doi:http://dx.doi.org/10.1098/rsta.2012.0421.
[32] Masters I, Malki R, Williams AJ, CroftCroft TN. The influence of flow acceleration on tidal stream turbine wake dynamics: a numerical study using a coupled BEM-CFD model. Appl Math Model 2013;37(16–17):7905–18. http://dx.doi.org/10.1016/j.apm.2013.06.004.
[33] Batten W, Bahaj A, Molland A, Chaplin J. Hydrodynamics of marine current turbines. Renew Energy 2006;31(2):249–56. http://dx.doi.org/10.1016/j.renene.2007.05.043.
[34] Lee SH, Lee SH, Jang K, Lee J, Hur N. A numerical study for the optimal arrangement of ocean current turbine generators in the ocean current power parks. Curr Appl Phys 2010;10(2):S137–41. http://dx.doi.org/10.1016/j.cap.2009.11.018.
[35] Belloni C, Willden R. Flow field and performance analysis of bidirectional and open-centre ducted tidal turbines. In: 9th European wave and tidal energy conference; 2011.
[36] Churchfield M, Li Y, Moriarty P. Flow field and performance analysis of bidirectional and open-centre ducted tidal turbines. In: 9th European wave and tidal energy conference; 2011.
[37] Nishino T, Willden R. Effects of 3-D channel blockage and turbulent wake mixing on the limit of power extraction by tidal turbines. Int J Heat Fluid Flow 2012;37:123–35. http://dx.doi.org/10.1016/j.ijheatfluidflow.2012.05.002.
[38] McAdam R, Houlsby G, Oldfield M, McCulloch M. Experimental testing of the transverse horizontal axis water turbine. Renew Power Gener IET 2010;4(6):510–8.
[39] Garrett C, Greenberg D. Predicting changes in tidal regime: the open boundary problem. J Phys Oceanogr 1977;7(2):171–81 doi:http://dx.doi.org/10.1175/1520-0485(1977)007<0171:PCITRT>2.0.CO;2.
[40] Carter GS, MAM. Open boundary conditions for regional tidal simulations. Ocean Model 2007;18(3–4):194–209. doi:http://dx.doi.org/10.1016/j.ocemod.2007.04.003.
[41] Adcock TAA. The open boundary problem in tidal basin modelling with energy extraction. In: 9th European wave and tidal energy conference. Southampton; 2011.
[42] Divett T, Vennell R, Stevens C. Optimization of multiple turbine arrays in a channel with tidally reversing flow by numerical modelling with adaptive mesh. Philos Trans R Soc A: Math Phys Eng Sci 2013;371(1985). http://dx.doi.org/10.1098/rsta.2012.0251 20120251–20120251.
[43] Funke SW, Farrell PE, Piggott MD. Tidal turbine array optimisation using the adjoint approach. Renew Energy 2014;63:658–73. http://dx.doi.org/10.1016/j.renene.2013.09.031.
[44] Divett T, Vennell R, Stevens C. Channel scale optimisation of large tidal turbine arrays in packed rows using large eddy simulations with adaptive mesh. In: Proceedings of 2nd Asian wave tidal energy conference, Tokyo; 2014.
[45] Draper S, Houlsby G, Oldfield M, Borthwick A. Modelling tidal energy extraction in a depth-averaged coastal domain. Renew Power Gener IET 2010;4(6):545–54. http://dx.doi.org/10.1049/iet-rpg.2009.0196.

[46] Karsten R, Swan A, Culina J. Assessment of arrays of in-stream tidal turbines in the bay of fundy. Philos Trans R Soc A: Math Phys Eng Sci 1985. http://dx.doi.org/10.1098/rsta.2012.0189.
[47] Betz A. Das Maximum der theoretisch möglichen Ausnutzung des Windes durch Windmotoren. Gesamte Turbinenwesen 1920;17:307–9.
[48] Lanchester FW. A contribution to the theory of propulsion and the screw propeller. Trans Inst Naval Archit 1915;LVII:98–116.
[49] Walters RA, Tarbotton MR, Hiles CE. Estimation of tidal power potential. Renew Energy 2013;51(25):5e262. http://dx.doi.org/10.1016/j.renene.2012.09.027.
[50] Plew DR, Stevens CL. Numerical modelling of the effect of turbines on currents in a tidal channel, Tory Channel, New Zealand. Renew Energy 2013;57:269–82. http://dx.doi.org/10.1016/j.renene.2013.02.001.
[51] Houlsby G, Draper S, Oldfield M, et al. Application of linear momentum actuator disc theory to open channel flow. Technical report; 2008.
[52] Bahaj A, Myers L. Shaping array design of marine current energy converters through scaled experimental analysis. Energy 2013;59:83–94. http://dx.doi.org/10.1016/j.energy.2013.07.023.
[53] Corten G. Heat generation by a wind turbine. In: 14th IEA symposium on the aerodynamics of wind turbines, vol. ECN report ECN-RX-01-001. National Renewable Energy Laboratory, USA; 2000. p. 7.
[54] Bryden IG, Grinsted T, Melville GT. Assessing the potential of a simple tidal channel to deliver useful energy. J Appl Ocean Res 2004;26:198–204. http://dx.doi.org/10.1016/j.apor.2005.04.001.
[55] MacLeod A, Barnes S, Rados K, Bryden I. Wake effects in tidal current turbine farms. In: International conference on marine renewable energy-conference proceedings; 2002. p. 49–53.
[56] Malki R, Masters I, Williams AJ, Croft TN. Planning tidal stream turbine array layouts using a coupled blade element momentum—computational fluid dynamics model. Renew Energy 2014;63:46–54. http://dx.doi.org/10.1016/j.renene.2013.08.039.
[57] Mycek P, Gaurier B, Germain G, Pinon G, Rivoalen E. Numerical and experimental study of the interaction between two marine current turbines. Int J Mar Energy 2013;1:70–83. http://dx.doi.org/10.1016/j.ijome.2013.05.007.
[58] Huang H-S. Efficient hybrid distributed genetic algorithms for wind turbine positioning in large wind farms. In: 2009 IEEE international symposium on industrial electronics. Institute of Electrical and Electronics Engineers; 2009. p. 2196–201. doi:http://dx.doi.org/10.1109/ISIE.2009.5213603.
[59] Zingg DW, Nemec M, Pulliam TH. A comparative evaluation of genetic and gradient-based algorithms applied to aerodynamic optimization. Eur J Comput Mech/Rev Eur Méc Numér 2008;17(1–2):103–26. http://dx.doi.org/10.3166/remn.17.103-126.
[60] Manwell J, McGowan J, Rogers A. Wind energy explained. Sussex, UK: Wiley Online Library; 2002.
[61] Stansby PK. Limitations of depth-averaged modeling for shallow wakes. J Hydraul Eng 2006;132(7):737–40. http://dx.doi.org/10.1061/(ASCE)0733-9429(2006)132:7(737).
[62] Vennell R, Old CP. High resolution observations of the intensity of secondary circulation along a curved tidal channel. J Geophys Res 2006;112:C11008. http://dx.doi.org/10.1029/2006JC003764.
[63] Karsten R, McMillan J, Lickley M, Haynes R. Assessment of tidal current energy in the Minas Passage, Bay of Fundy. Proc Mech Eng: Part A J Power Energy 2008;222(5):493–507. http://dx.doi.org/10.1243/09576509JPE555.
[64] Atwater JF, Lawrence GA. Power potential of a split tidal channel. Renew Energy 2010;35(2):329–32. http://dx.doi.org/10.1016/j.renene.2009.06.023.
[65] Polagye B, Malte P. Far-field dynamics of tidal energy extraction in channel networks. Renew Energy 2010;36(1):222–34. http://dx.doi.org/10.1016/j.renene.2010.06.025.
[66] Draper S, Adcock TAA, Borthwick AG, Houlsby GT. An electrical analogy for the Pentland Firth tidal stream power resource. Proc Soc R Soc Part A 2014;470(2161). http://dx.doi.org/10.1098/rspa.2013.0207 20130207.
[67] Funke S. Open tidal farm; 2013. URL ⟨http://opentidalfarm.org⟩.